6-23-2010

Synthesis and Characterization of Novel Nanomaterials: Gold Nanoshells with Organic-Inorganic Hybrid Cores

Alisha D. Peterson
University of South Florida

Synthesis and Characterization of Novel Nanomaterials: Gold Nanoshells with Organic-Inorganic Hybrid Cores

by

Alisha D. Peterson

A thesis submitted in partial fulfillment
of the requirements for the degree of
Master of Science in Engineering Science
Department of Chemical and Biomedical Engineering
College of Engineering
University of South Florida

Major Professor: Vinay K. Gupta, Ph.D.
John T. Wolan, Ph.D.
Mark Jaroszeski, Ph.D.

Date of Approval:
June 23, 2010

Keywords: thermally-responsive, poly N-isopropylacrylamide, optical absorption, metallic, multilayered nanomaterial

DEDICATION

This thesis is dedicated to my entire loving and supportive family.

To the influential women in my life:

My grandmother whose strength encourages me daily

My mother whose guidance keeps me moving forward in a positive direction

&

My sister whose constant encouragement helps me to reach all of my goals

ACKNOWLEDGEMENTS

I would first like to thank my advisor, Dr. Vinay Gupta, for his guidance, support and patients over the past two years. I would like to express gratitude to my committee members, Dr. John Wolan and Dr. Mark Jaroszeski, who have played an important role in my success as a graduate student. I would also like to thank my lab partners who have all helped me succeed in one way or another: Mr. Bijith Mankidy, Ms. Kristina Tran, and Ms. Fedena Fanord. Special thanks to Mrs. Yvonne Williams, Dr. Shekhar Bhansali and Mr. Bernard Batson for their constant support and guidance. Lastly, I would like to acknowledge the NSF Florida-Georgia Louis Stokes Alliance for Minority Participants (HRD#0929435) for financial support throughout my graduate career.

TABLE OF CONTENTS

LIST OF FIGURES

Synthesis and Characterization of Novel Nanomaterials: Gold Nanoshells with Organic-Inorganic Hybrid Cores

Alisha Peterson

ABSTRACT

Gold nanoshells, a material generally composed of a core of silica surrounded by a thin shell of gold, are of great interest due to their unique and tunable optical properties. By varying the shell thickness and core size, the absorption and scattering properties are greatly enhanced. The nanoshells can be made to absorb or scatter light at various regions across the electromagnetic spectrum, from visible to the near infrared. The ability to tune the optical properties of nanoshells allows for their potential use in many different areas of research such as optical imaging, tumor ablation, drug delivery, and solar energy conversion. The research in this thesis focused on the synthesis and characterization of two novel gold nanoshell materials containing thermally-responsive, organic-inorganic hybrid layers. One type of material was based on a two-layer particle with a thermally responsive hybrid core of N-isopropylacrylamide (NIPAM) copolymerized with 3-(trimethoxysilyl)propyl methacrylate (MPS) that was then coated with a thin layer of gold. The second material was a three-layer particle with a silica core, a thermally responsive copolymer of NIPAM and MPS middle layer and an outer shell of gold. Various techniques were used to characterize both materials. Transmission electron microscopy (TEM) was used to image the particles and dynamic light scattering

(DLS) was used to determine particle size and the temperature response. Additionally, UV-Vis spectroscopy was used to characterize the optical properties as a function of temperature.

CHAPTER 1: INTRODUCTION AND BACKGROUND

1.1 Traditional Metallic Nanoshells

Gold nanoshells are of great interest due to their nanosized dimensions and uniquely tunable optical properties. Their ability to absorb and scatter light in the visible and near-infrared regions stems from collectively oscillating conduction electrons stimulated by the electric field in the incident beam [1-3].

For isotropic colloidal gold nanoparticles, localized surface plasmon resonance is seen only in the visible region and is typically around 520 nm for isolated particles between 10-20 nm. Changing the shape or attaching spherical particles to a larger colloidal substrate, forming nanoshells, allows the optical properties to be easily tuned to various ranges across the electromagnetic spectrum [1, 4]. For example, nanorods are elongated nanoparticles that display two plasmon bands, as opposed to the single band seen in spherical nanoparticles. There is a transverse band in the visible and a longitudinal band located in the near infrared region (> 700 nm). The exact location of the longitudinal band depends on the aspect ratio of the elongated nanorods [3, 5]. In the case of gold nanoshells, where the gold nanoparticles are attached to a large colloidal core of a dielectric material, the coupling of localized surfaced plasmons for the nanoparticles that make up the shell leads to absorption in the near infrared region. Silica and polystyrene are commonly used as colloidal substrates for traditional gold nanoshells. Polystyrene has a low decomposition temperature and a high solubility rate in most

commonly used solvents. These characteristics make polystyrene ideal for creating hollow gold nanoshells. Silica is often used because it is chemically inert, optically transparent, and structurally stable against degradation and coagulation. Therefore, it is used most often to build two layered gold nanoshells. Many techniques have been studied to deposit gold nanoparticles onto the surface of silica and polystyrene. Synthesis methods including, sol-gel condensation, layer by layer (LBL), and deposition precipitation (DP) have been developed to construct both hollow and two-layered metallic nanostructures [2, 6-10].

Gold nanoshells are optically versatile, capable of both absorbing and scattering electromagnetic radiation at various wavelengths. Their scattering abilities are great for use in optical imaging applications and absorption properties give gold nanoshells the ability to convert light energy into heat, namely photothermal conversion. Photothermal conversion has been studied for a variety of biomedical applications. Exploration of both absorption and scattering properties of gold nanoshell will greatly benefit many different applications including, drug delivery systems, cancer treatment, and solar energy conversion [2, 5, 7, 11].

The overall goal of this research is to develop gold nanoshells constructed with organic-inorganic hybrid cores. The use of hybrid cores will enhance the tunability of the metallic nanoshells optical properties since it provides a versatile route to controlling the dielectric core. In addition, the use of organic polymers such as PNIPAM can lead to novel effects since the cross-linked PNIPAM matrix is capable of swelling and collapsing in response to thermal stimulus. Thus, by using temperature responsive polymeric layers

to create metallic nanoshells one can tune the optical properties of metallic nanoshells during and after the synthesis process.

1.1.1 Synthesis of Traditional Gold Nanoshells

Although several methods [2, 7, 9, 12] have been used to synthesize gold nanoshells, two of the most popular methods will be described in this section. One method uses multiple steps to separately synthesize and functionalize each component, then combine them into one particle in a final step. Here, this method is referred to as layer-by-layer technique (LBL) [6, 9, 13, 14]. Deposition-precipitation (DP) is an alternative, and sometimes favored, route to produce traditional gold nanoshells [7, 15, 16]. The DP process is sometimes preferred because it minimizes the number of steps used, which ultimately makes the synthesis process shorter. Despite the fact that the deposition-precipitation method is shorter, controlling every parameter, such as pH, temperature, and reaction time, needed to make the synthesis a success can be difficult. Therefore, it is sometimes necessary to take the longer LBL route to achieve desired results. Figure 1.1 shows step by step schematic of the synthesis process for silica core gold nanoshells.

The first two steps of either method, LBL or DP, are the same. First, the core particle is synthesized and then in a second step, its surface is modified. Synthesizing silica is most commonly done using the well-known Stöber method developed by Werner Stöber and Arthur Fink in the 1960s [17]. This method uses ammonium hydroxide as a catalyst in a hydrolysis-condensation reaction of tetraethylorthosilicate (TEOS). Hydrolysis is the first step of the Stöber method wherein the ethoxy groups are replaced

with hydroxyl groups. The second step is polycondensation, where water is removed from the silicon hydroxide groups to form silicon dioxides (SiO_2). Figure 1.2 shows the mechanism of this reaction. By varying one or more of the reaction parameters the size, porosity and morphology can be altered as desired. Altering the concentrations of TEOS, ammonium hydroxide, and even the total reaction volume produces different sized particles. Varying the ammonium hydroxide concentration also alters the porosity and morphology of the silica [2, 17]. Experiments discussed in chapters 1 show that manipulating the reaction temperature as well as the total reaction time also played a major role in the size of the particles produced.

The second step in the LBL or DP processes is the modification of the silica surface. Surface modifiers are often used to alter the surface charge of silica. Varying the surface charge promotes the attachment of additional materials to the silica surface. Many functional groups have been studied for the purpose of surface modifying silica particles. Amine (-NH2), thiol (-SH), and vinyl (-C=C) groups are among some of the most commonly used functional groups [15, 18-22]. Determining the appropriate group to use depends on the species that is to be attached to the silica surface. For instance, vinyl groups are often used as surface modifiers to induce the growth of polymeric chains on silica surfaces. In this case, an initiator is used for free radical polymerization of a monomer and grafting of the polymer to the silica surface [23, 24].

For gold nanoshells, it is necessary to attach gold nanoparticles to the silica surface. To achieve this, reagents bearing positively charged amine groups, such as 3-aminopropyltrimethoxysilane (APTMS) or 3-aminopropyltriethoxysilane (APTES) are commonly used as coupling agents on the silica surfaces [2, 6, 7, 11, 16, 25]. Although

literature methods exist [16, 26] where surface modification is not necessary to attach metallic nanoparticles, the use of surface modified cores ensures the attachment of metallic particles in a dense manner [2, 16]. The reason for this difference lies in the fact that the isoelectric point (IEP) or point of no electric charge of bare silica is ~2. Above the IEP the surface charge of silica is negative, which makes it difficult for negatively charged gold nanoparticles to attach to its surface [7, 27]. There have been reports where the IEP of silica was manipulated, to alter the surface charge, through prolonged exposure to various solutions. For example, ammonium hydroxide used during silica synthesis, can shift the surface charge from negative to positive, if used in excess amounts. Positively charged ammonia cations attach to the silicon hydroxide species which eliminates the need for an additional APTMS or APTES functionalization step [16, 26, 27].

The layer-by layer (LBL) method involves, synthesizing and surface modifying the core silica particles, as described previously, followed by the synthesis and attachment of gold nanoparticles, and lastly the growth of the metallic shell around the core. Gold nanoparticles, ~2nm in size, are synthesized by reducing a solution of tetrachloroauric acid ($HAuCl_4$) in an aqueous medium. Gold ions precipitate into metallic gold nanoparticles by using reducing agents such as, formaldehyde, sodium borohydride, sodium hydroxide, or ascorbic acid [2, 6, 7]. This process often incorporates a capping agent, sodium citrate or tetrakis (hydroxymethyl) phosphonium chloride (THPC), to stabilize the nanoparticles and prevent aggregation [28] Gold nanoparticles are then attached to the surface modified silica; this is known as core

seeding. The metallic nanoparticles serve as nucleation sites to promote further reduction of gold salt in the form of a shell.

There are three key ingredients used in the gold shell growth process. The first is a gold solution known as K-Gold, it consists of tetrachloauric acid and potassium carbonate mixed in an aqueous medium. Silica core particles are dispersed in this solution prior to shell growth. Next a reducing agent, commonly sodium borohydride or formaldehyde, is used to reduce the gold in the K-Gold solution from Au^{3+} to Au^{0}. The gold seeds on the core surface will attract the additional reduced gold, from the K-Gold solution, to form a layer around the silica surface. Prior to adding the reducing agent, a capping agent is added to slow the reaction and stabilize the particles [6, 7, 13, 25].

In order to seed the silica core particles without separately synthesizing gold nanoparticles the deposition precipitation (DP) method is used. The DP method is commonly used for synthesis of catalytic oxide materials, but Phonthammachai and coworkers have demonstrated the use of this method to seed silica particles with gold nanoparticles [7, 16, 26]. Here, gold salt solution is hydrolyzed in the presence of amine functionalized silica particles under slightly basic conditions, pH 7-9. Basic conditions are necessary because at this pH range the more prevalent gold anions are $(Au(OH)_3Cl)^-$, and precipitation is most efficient using this specious of chloroauric anions. Also, a basic pH is above the IEP of the support material, as a result negatively charged chloride ions are not attracted to its surface. The inability for chloride ions to attach to the silica surface encourages the growth of favorably small gold nanoparticles [7, 29, 30]. After seeding, the shell is grown using the same method described previously in the section for the LBL method, using K-Gold, reducing agents, and capping agents [7].

1.1.2 Optical Properties of Gold Nanoshells

The properties of metallic nanoshells include, but are not limited to, optical, magnetic, photothermal, and catalytic [2, 31-33]. The coating material used for shell formation determines which of these properties will be exhibited. For nanoshells coated with gold, photothermal and optical properties, consisting of light absorption and scattering are most commonly displayed. The expression of optical properties or ability for gold nanoshells to scatter or absorb light is based on what is called surface plasmon resonance [2, 3, 34, 35]. In metal films, plasmons are described as positively charged clouds of ions and negatively charged clouds of electrons overlapping one another. Disturbance, from external radiation, causes the electron cloud to become polarized. To reinstate equilibrium, the electrons will generate kinetic energy, which causes the conduction electrons to exceed their steady state value. The excitation of the electrons causes them to collectively oscillate at a particular frequency. For spherical gold nanoparticles the electrons are localized only on the outer surface causing the electron oscillations to be seen only in the visible region, ~520nm. In gold nanoshells the coupling of LSPR can be shifted to the near infrared region, between 800-1200 nm as a result of interactions between the electrons of the two, inner and outer, surfaces of the shell. These oscillation patterns are shown in figure 1.3. Varying the shell thickness during synthesis determines how much of how little the electrons of the two surfaces interact. [2, 3, 12, 33, 35-38]. Literature studies have shown that there is a red shift, towards the NIR region, in the LSPR band if the shell thickness is less than the radius of the core particle. If the shell thickness is greater than the core radius a blue shift towards the visible region is observed. The absorbance shift is illustrated later in this thesis in

chapter two, figure 2.7. This trend is only considered feasible if the gold nanoshell is coated in a uniform manner around the entire core particle [12]. In short, as the number of gold nanoparticles on the silica surface increase there is a red shift, towards the NIR region, but once the shell thickens particle separation is increased and the coupling between particles is suppressed and a blue shift is detected [2, 39].

Determining particle size and optical properties are very important when deciding which applications will benefit most from the use of gold nanoshells. The detection of optical absorption, scattering and photothermal properties, of gold nanoshells has been well studied [1, 12, 39-41]. These properties can be easily characterized using UV-vis spectroscopy. Typically, nanoshells are dispersed in an aqueous or organic medium and UV-vis spectroscopy is used to characterize the optical extinction of gold nanoshells. Photothermal properties of nanoshells have been tested by NIR laser irradiation of an aliquot of nanoshell solution in a small amount of water and measurement of the temperature change by using a thermocouple [33].

1.1.3 Applications of Gold Nanoshells

Due to the unique optical properties of gold nanoshells, they have been explored for a variety of potential applications [3, 4, 42-45]. Among these potential applications, most attention has focused on cell imaging, photothermal ablation, and drug delivery. The popularity of metallic nanoshells for use in biomedical applications is due to the fact that biological tissue penetration is possible, without damage, at NIR wavelengths. In this region gold nanoshells are able to absorb or scatter light efficiently. This material also offers a, cheap, minimally invasive method to investigate biological tissues [42].

The optical scattering properties of metallic nanoshells have been studied to enhance current tissue imaging techniques. For example, using a dark field microscope white light can be used to excite the conduction electrons causing scattering to occur at a distinct frequency. Through the use of biomarkers, the particles can be attached to one desired cell type, and when the nanoshells are illuminated the attached cells can be easily imaged [11, 46]. Photothermal tumor ablation is another biomedical application of great interest. Ablation of cancerous tissue is achieved by first attaching the nanoshells to the cells through the use of biomarkers and then applying a radiation source. The localized heating causes destruction to cancerous tissue in the proximity of the nanoshells. This technique is beneficial because it allows for healthy cells to remain un-affected [11, 42, 46-48].

Although, biomedical applications seem to dominate the research surrounding gold nanoshells, a few theoretical studies have been completed to determine the ability of gold nanoshells to be used in harvesting and conversion of solar energy [4, 49]. Incorporating gold nanoshells into building structures, through the use of coatings or paints, can greatly reduce the amount of electricity used for heating, both industrially and domestically. Using gold nanoshells to convert solar energy for heating purposes will greatly advance the search to find alternative energy methods. Gold nanoshells can be optically tuned to absorb or scatter light at a desired wavelength or across various region of the solar spectrum. The sun emits half of its light in the visible region 400-700 nm, where gold nanoparticles are great absorbers, and the other half at longer NIR wavelengths, that cannot be absorbed or scattered by existing materials. This void can be met through the use of tunable gold nanoshells [49]. Using the Mie theory, an optimal

combination of gold nanoshells and gold nanoparticles can be determined that would allow for the absorption or scattering of most of the solar spectrum [4, 36].

1.2 Project Summary

This thesis focuses on the development and characterization of novel gold nanoshells capable of absorbing light across the electromagnetic spectrum. As described earlier, traditional gold nanoshells offer tunable optical properties via changes in the geometry of the shell relative to the core, which is controlled during the synthesis process. In this research project, we have focused on a material that provides a different level of versatility by combining organic materials with inorganic components for the core. Because the core polymeric material consists of a thermally responsive polymer, the optical properties can also be manipulated using an external stimulus such as temperature.

The thesis is organized as follows. Chapter 2 focuses on the traditional gold nanoshells that were synthesized in our lab for comparison with the novel hybrid materials. Chapter 3 discusses the synthesis and characterization of a two-layer gold nanoshell and Chapter 4 presents the work on a three-layer gold nanoshell material. Chapter 5 of the thesis provides a summary of the research results.

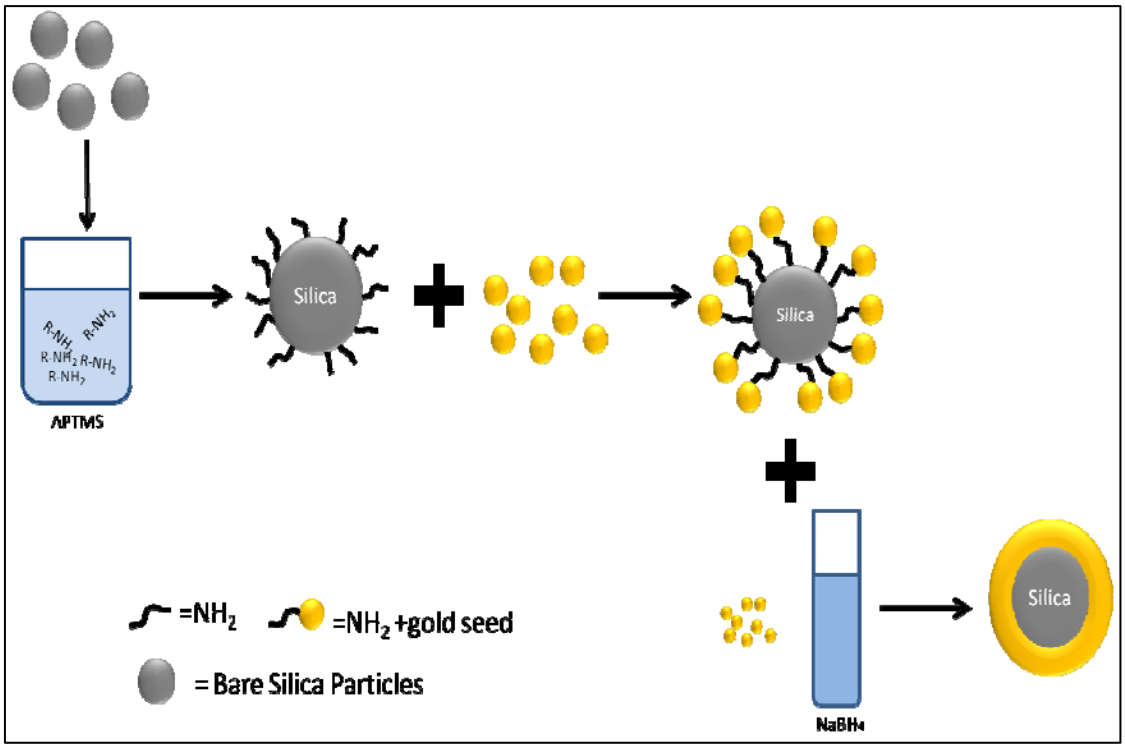

Figure 1.1: Schematic of the LBL synthesis of traditional gold nanoshells.

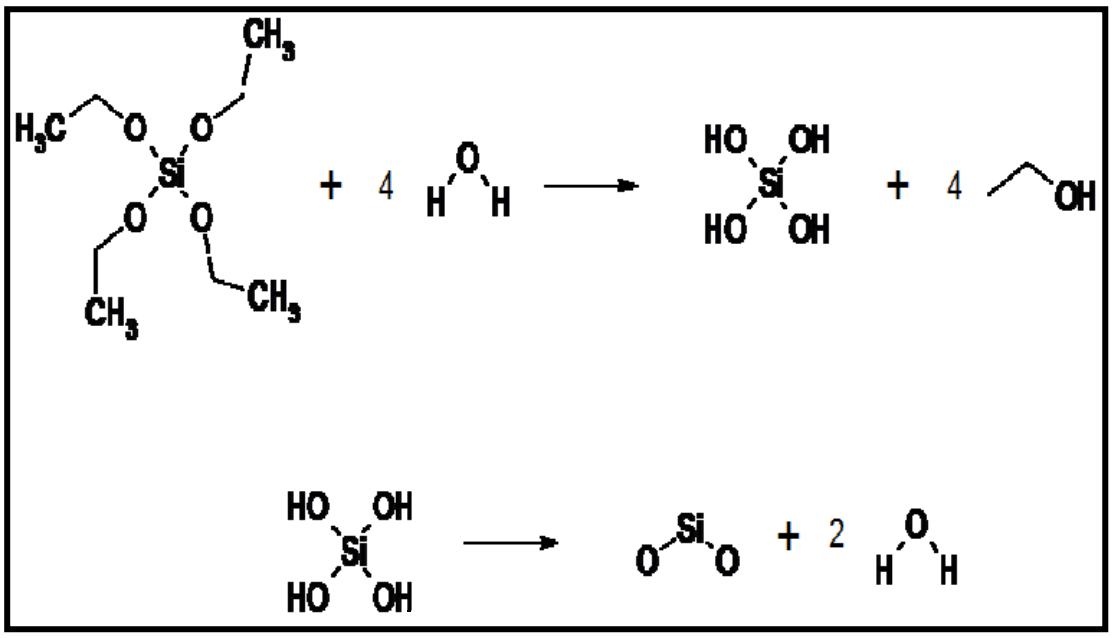

Figure 1.2: Synthesis scheme for Stöber silica particles.

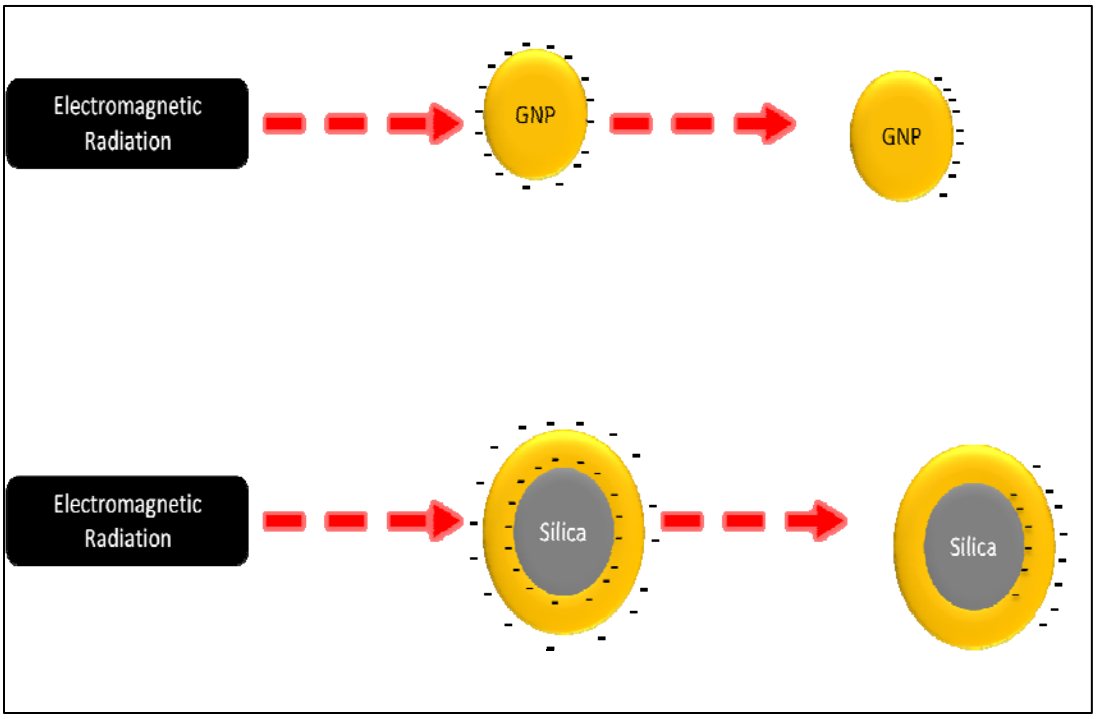

Figure 1.3: Electronic charge displacement of gold nanoparticles (GNP) (top) compared to gold nanoshells (bottom) due to the electric field of incident radiation.

CHAPTER 2: SYNTHESIS AND CHARACTERIZATION OF TRADITIONAL GOLD NANOSHELLS

2.1 Synthesis and Functionalization of Stöber Silica

Traditional gold nanoshells were synthesized and characterized for comparison against two and three layered hybrid gold nanoshells. These particles were prepared using the deposition precipitation method [7, 16]. This method involved the synthesis of a silica core particles, using the Stöber method, that were amine ($-NH_2$) terminated through surface modification with 3-aminopropyltrimethoxysilane (APTMS). Amine groups bear a positive charge that helps in the attachment of negatively charged gold nanoparticles. The amount of APTMS added must be sufficient enough to coat the entire surface of each particle; therefore, it was added in excess. Functionalized core particles were then seeded in one step using a basic gold solution and the shell was grown using a strong reducing agent, namely $NaBH_4$.

2.1.1 Experimental

- Materials: Ammonia hydroxide (28-30%) was purchased from Sigma Aldrich. Tetra ethyl orthosilicate (TEOS 98%) and 3-aminopropyltrimethoxysilane were both purchased from Acros Organics and ethanol from Pharmaco-AAPER & Commercial Alcohols. Deionized water was purified using an Easypure UV water system.

- Stöber Silica: In a 200mL round bottom flask, 10mL of water and 5mL of ammonium hydroxide were added to 100mL of ethanol and vigorously mixed at 30^{o}C for 30minutes. 6mL of TEOS was then added and the reaction was continued, undisturbed overnight, ~24 hours. To remove the particles from the ethanol medium they were centrifuged and washed using water in a series of centrifugations. After purification the particles were dried for a minimum of 6 hours in a vacuum oven and weighed.
- Surface Modification: To functionalize the surface of the silica particles APTMS was used. 200mg of the dried bare particles were redispersed, using sonication, in 10mL of toluene. The turbid solution was then added to a 25mL round bottom flask and placed in a 75^{o}C oil bath. An excess of APTMS, 65uL, was added to the solution and the reaction continued with mixing for 12 hours. Amine functionalized silica particles were purified to remove any un-reacted APTMS. To accomplish this centrifugation was used. They were first centrifuged to remove the original medium, redispersed and centrifuged twice in toluene. This was followed by four washes in ethanol to remove any excess toluene and four washes in water to remove any remaining ethanol. Lastly, surface modified silica particles were dried in a vacuum oven overnight.
- Characterization Techniques: Dynamic light scattering (DLS) was carried out using a Malvern Zetasizer Nano-S instrument. DLS investigated the size distribution of the silica particles. Sample preparation included, dispersing 20uL of particle solution in 1mL of water inside of a 2mL polystyrene cuvette. FEI Morgagni 268D transmission electron microscope was used to image the particles

to determine the shape and polydispersity in size. For imaging, sample preparation included depositing and drying ~20uL of sample on a formvar copper grid. A Nicolet Magna IR Spectrometer 860 was used characterize the silica particles. The samples were prepared by mixing dried silica particles with potassium bromide (KBr) and crushing the powder to form a pellet.

2.1.2 Results and Discussion

Silica core particles were successfully prepared by mixing TEOS at a warm temperature of 30^{o}C for a 24 hour period. Heating the solution and prolonging the reaction time resulted in the production of small nanoparticles below 200nm in diameter. For size comparison, additional silica particles were made using the same Stöber method but the reaction was done at room temperature and the time was reduced to 6 hours. DLS size distribution graphs shown in figure 2.1 compares the difference in silica size based on reaction time and temperature. For those particles synthesized at 30^{o}C the diameter is measured to be ~190nm. By slightly altering the reaction time and temperature as discussed previously, the particle diameter was doubled to ~390nm. TEM images of bare silica, shown in figure 2.2, confirm that the particles prepared at 30^{o}C are less than 200nm in diameter and have low polydispersity in size.

Images of amine functionalized silica particles are almost identical to those of bare silica particles indicating that the APTMS functionalization does not lead to aggregation. FTIR spectrum was used to characterize the presence of APTMS on silica particles. Figure 2.3 shows the IR spectra, which are dominated by the Si-O-Si peak around 1000cm^{-1}. The spectrum of the amine functionalized silica particles revealed no

significant peaks from the organic molecules; presumably the small amount of APTMS on the surface was not sufficient for detection by IR absorption. The indication of amine presence on silica surfaces was later evident through the production of evenly coated gold nanoshells that are described in the next section.

2.2 Gold Nanoshells Using Deposition Precipitation Method

As discussed earlier, the DP process is a synthesis technique favored because it uses fewer steps than most other methods. This method avoids the excess step of synthesizing an additional gold nanoparticle solution. Instead, the nanoparticles are precipitated in the presence of amine functionalized silica particles. Several different K-gold solution to core particle solution ratios were used when synthesizing traditional gold nanoshells to achieve a different shell thicknesses

2.2.1 Experimental

- Materials: Chloroauric acid ($HAuCl_4 \cdot 3H_2O$ 99%) was purchased from Sigma Aldrich, sodium hydroxide and potassium carbonate were both purchased from Fischer Scientific, and lastly sodium citrate and sodium borohydride (98%) were purchased from Acros Organics.
- DP Gold seeding of surface modified silica: Using sonication, 100mg of amine grafted silica particles were dispersed in 1mL of water. Separately, an aliquot of 0.1M NaOH was added drop by drop to 4mL of 6.35mM $HAuCl_4$ to adjust its pH to 8. The silica solution was added to the basic gold chloride solution and mixed vigorously in a 10mL round bottom flask at 75^{o}C. The reaction continued for

45minutes. The gold seeded silica particles were washed multiple times in water to remove any un-reacted gold, and finally redispersed in water.

- Gold shell growth: In a150mL amber glass bottle, 100mL of K-Gold solution was made by dispersing 1.5mL of 25mM HAuCl4 in 100mLof water and adjusting the pH through the addition of 60mg of K_2CO_3. For the 250:1 ratio of K-Gold to silica particles, 100mL of gold seeded silica solution was added to 25mL of K-Gold solution and mixed for 3 minutes to disperse the particles. Then, 1.25mL of capping agent, sodium citrate were mixed into the reaction for 2-3 minutes prior to the addition of 2.5mL of reducing agent, $NaBH_4$. For 300:1 and 400:1 ratios, the amount of seeded particle solution remained the same as in the case for 250:1. The amount of K-Gold was increased to 30mL for 300:1 and 40mL for 400:1. Capping and reducing agents were increased proportionately to the increase in K-gold solution. The ratio of K-gold to capping agent is 20:1 so, for 300:1 shell ratios, 1.5mL was used and for 400:1 ratios 2mL was used. As for the reducing agent, its ratio to K-gold is 10:1, therefore 3 and 4mL of $NaBH_4$ was used for 300:1 and 400:1 ratios, respectively.
- Characterization Techniques: FEI Morgagni 268D transmission electron microscopy was used for imaging the nanoparticles after seeding and final shell growth. UV-vis spectra were recorded using a Jasco V-530 UV/Vis Spectrophotometer. The spectra determined the light absorption pattern of the particles based on their shell thickness. Gold nanoshell deposition onto a formvar copper grid surface was the method of preparation for TEM grids and UV-vis

samples were prepared by simply adding 1mL of particle solution to a 2mL polystyrene cuvette.

2.2.2 Results and Discussion

Successful deposition of gold nanoparticles on silica cores was achieved by using the DP method. High temperature of 75^{o}C was used to promote bonding between the terminated amine groups on the silica surface and the gold nanoparticles. Basic conditions were used to ensure that the gold ions precipitated to form gold nanoparticles efficiently, and the total reaction time was limited to 45 minutes to prevent the formation of large gold clusters in solution and on the core surface [7, 16]. During shell growth, a capping agent, sodium citrate, was used to decrease the chances of aggregate formation and because $NaBH_4$ is a strong reducing agent, the sodium citrate also played a role in slowing the reduction reaction. Another way the reaction was slowed was to add the reducing agent ($NaBH_4$) in increments of 500uL every 20-30 seconds. TEM was used to image this material at both the seeding and shell growth steps. Images of gold seed silica particles are shown in figure 2.4. These images display silica particles with small gold nanoparticles, ~2-6nm, absorbed to their surfaces. Gold seeds 2-6nm in diameter are good for producing evenly coated gold nanoshells. The different gold nanoshells, with ratios of 250:1, 300:1, and 400:1, are shown in figure 2.5. Each of these nanoshell materials exhibit fairly uniform but incomplete shells. These particles were not highly aggregated and the shell thickness appeared to be the same for most of the particles found on the grid. The images of each sample, 250:1, 300:1, and 400:1, look very similar in appearance but a distinction between each can be seen in the UV-vis spectra presented in

figure 2.6. Each peak expands across the visible and near infrared regions from 600nm to 1000nm. As the K-gold to silica particle solution ratio increases the shell thickness increases. An increase in the shell thickness causes a red shift in the absorption band.

Results discussed in this chapter demonstrate that the traditional gold nanoshells were successfully prepared using the DP method and their characterization by UV-Vis and TEM provide the basis for comparison to the properties of the novel organic-inorganic hybrid nanoshells, discussed in the next two chapters.

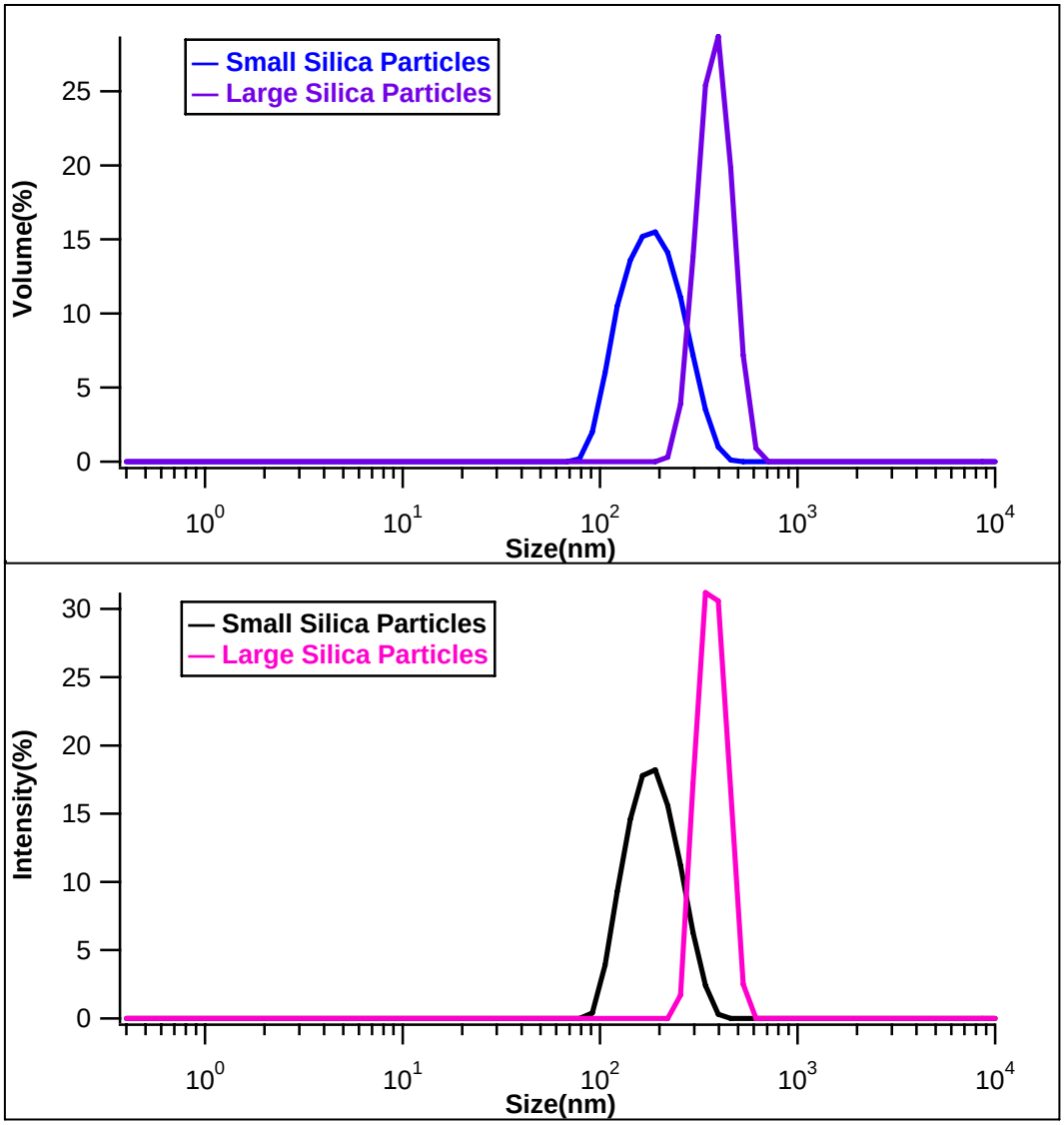

Figure 2.1: DLS measurements of large bare silica particles (~350nm) compared to small bare silica particles (~190nm). Both the volume distribution (top) and the intensity distribution (bottom) are shown.

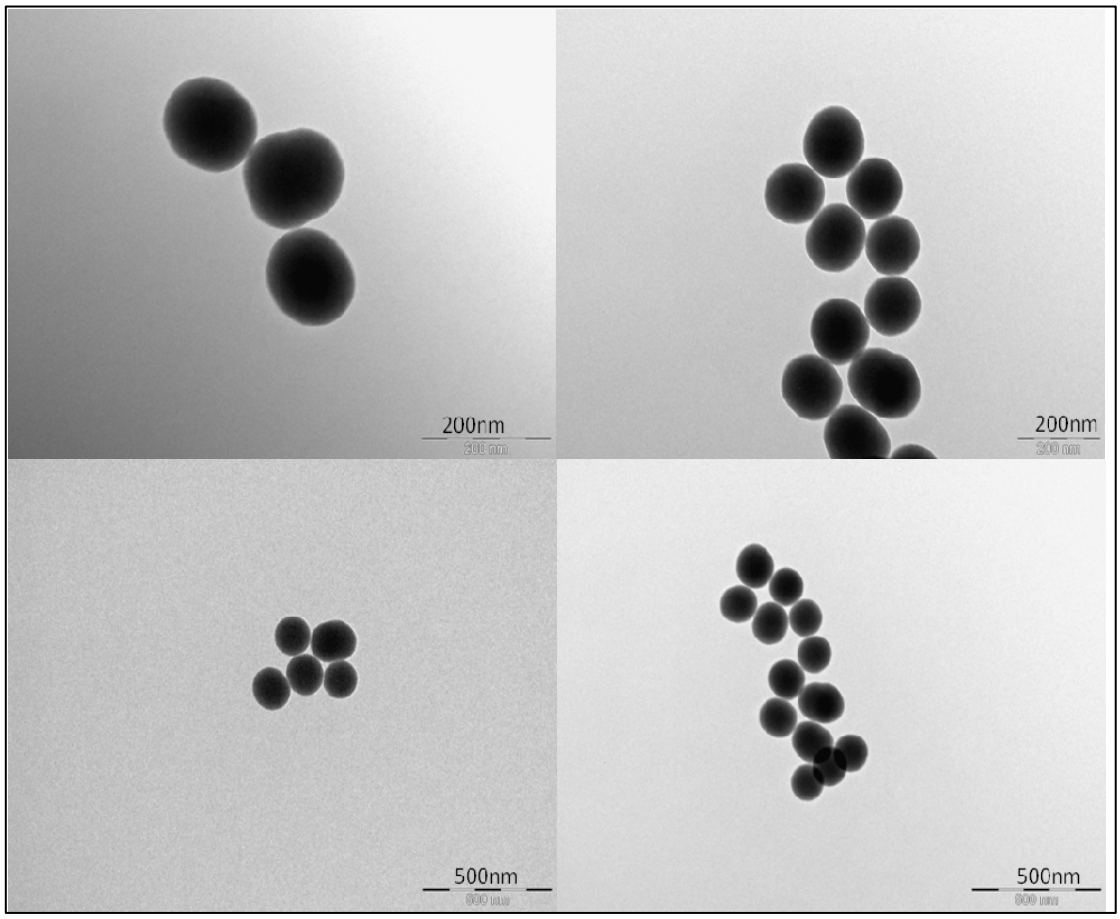

Figure 2.2: TEM images of bare silica particles with a mean size ~190nm.

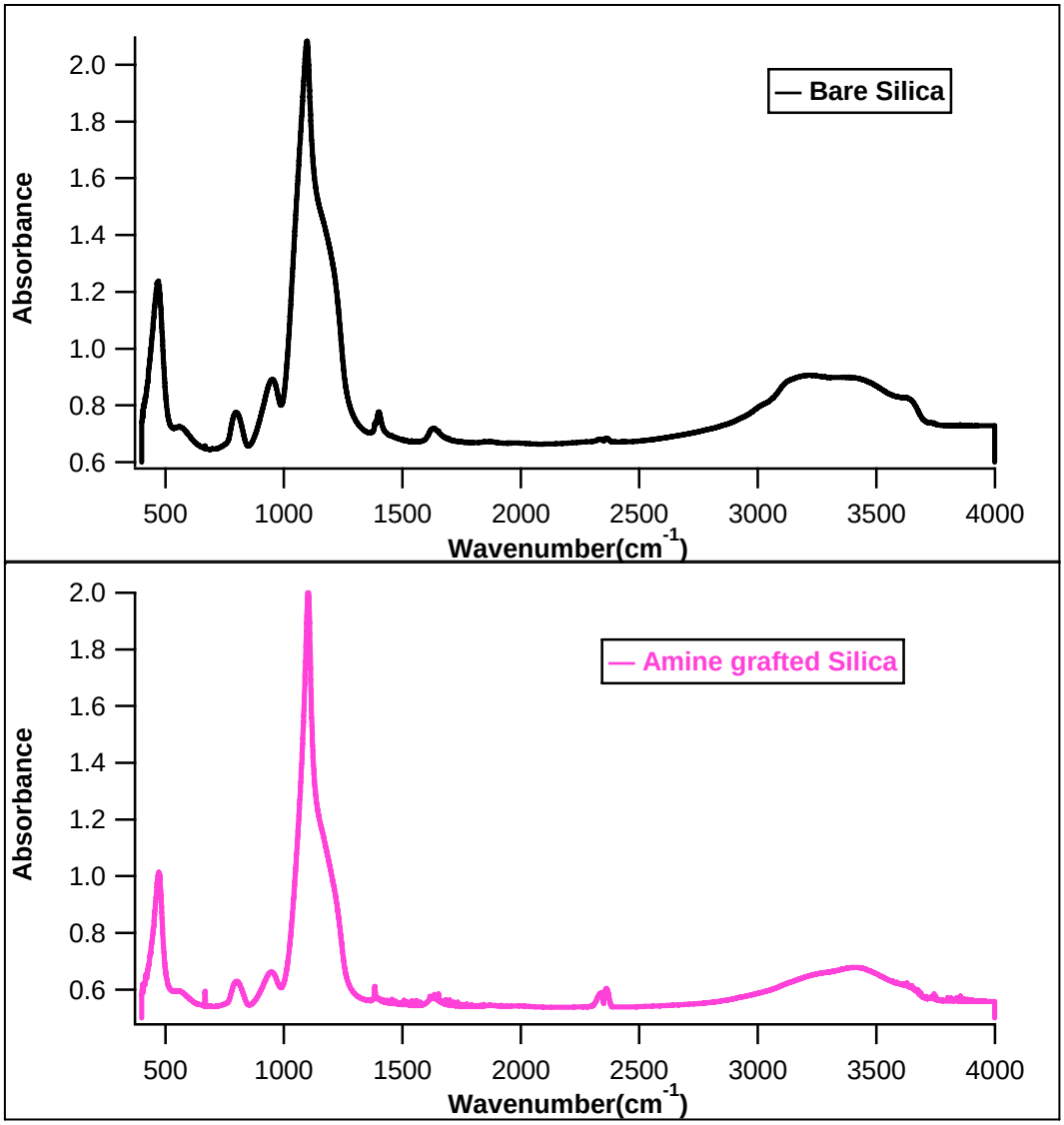

Figure 2.3: FTIR spectrum of bare silica (top) compared to IR spectrum of amine functionalized (bottom) silica particles.

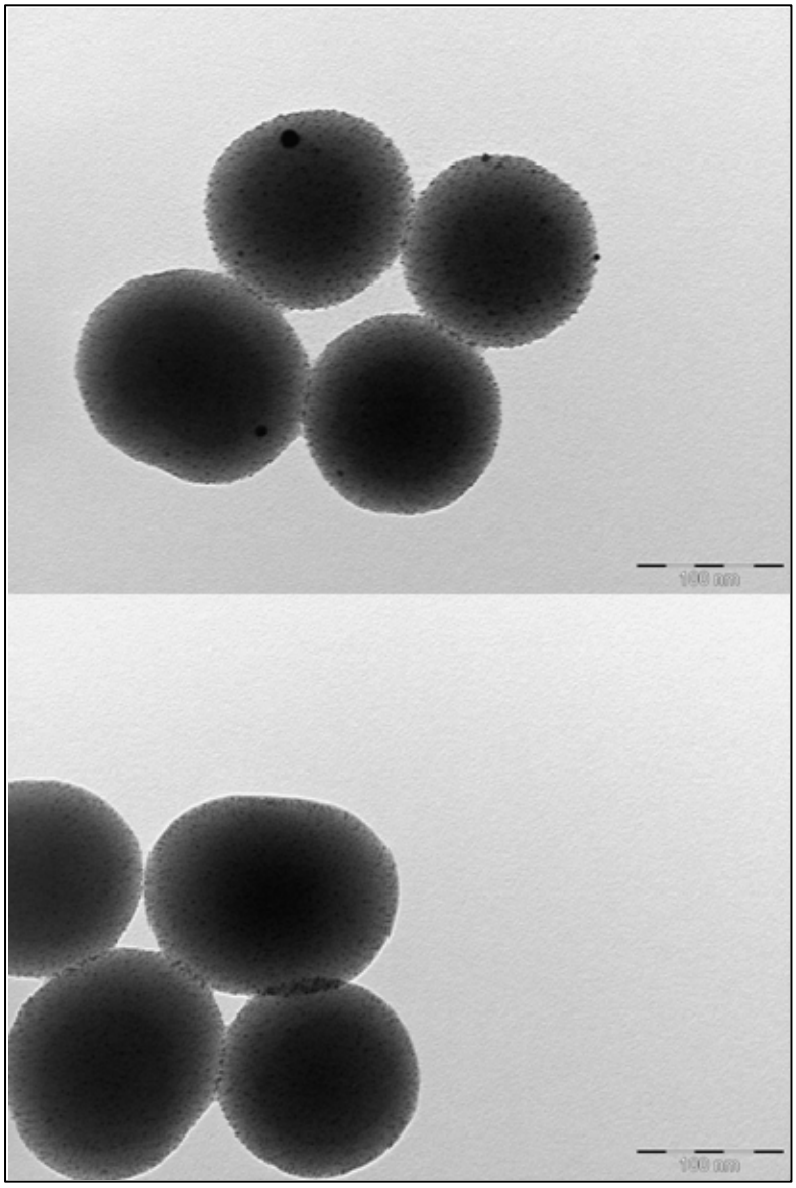

Figure 2.4: TEM images of gold seeded silica particles. In both images, the scale bar shown corresponds to 100nm.

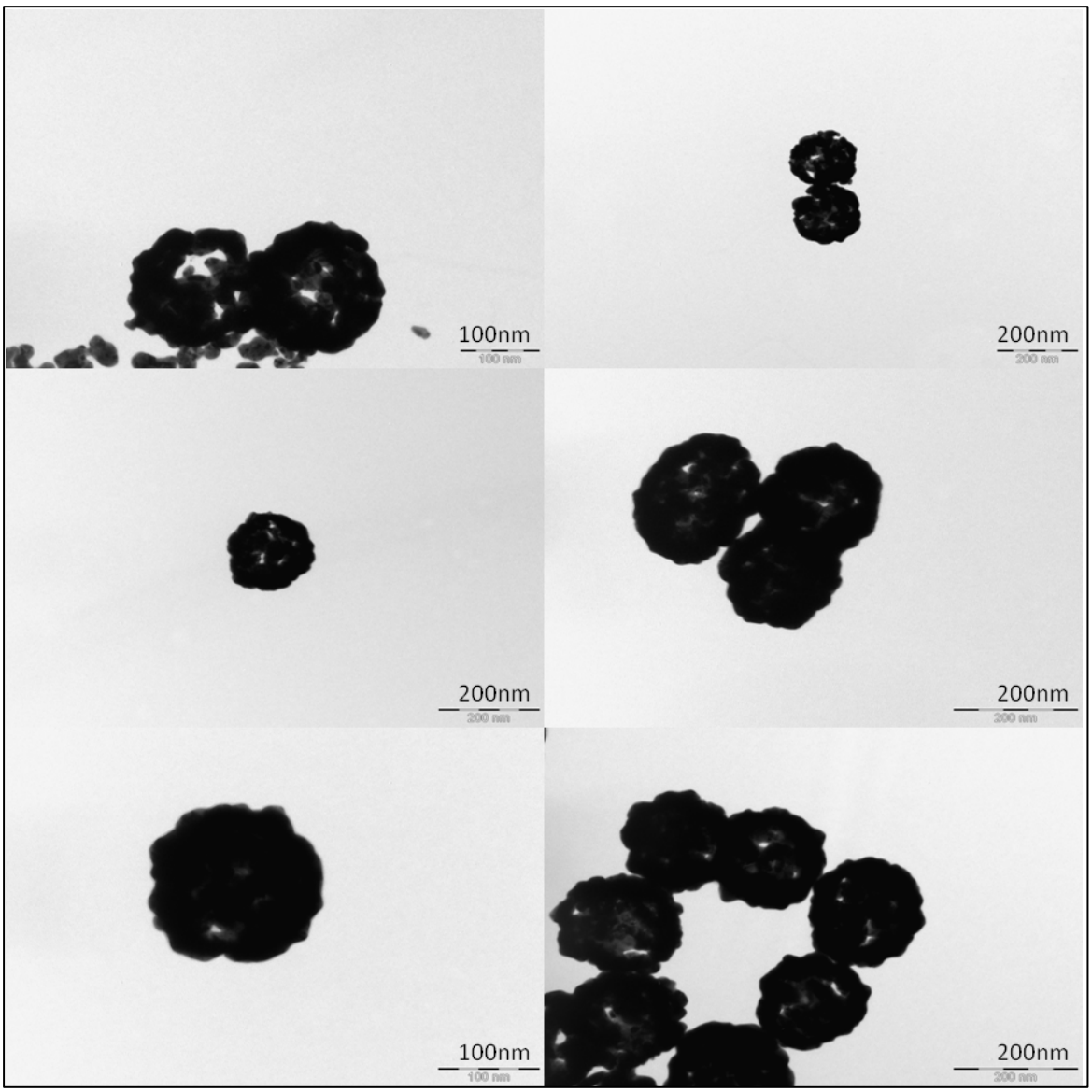

Figure 2.5: TEM images of gold nanoshells with different K-Gold to seed ratios. 250:1 (top), 300:1 (middle), and 400:1 (bottom).

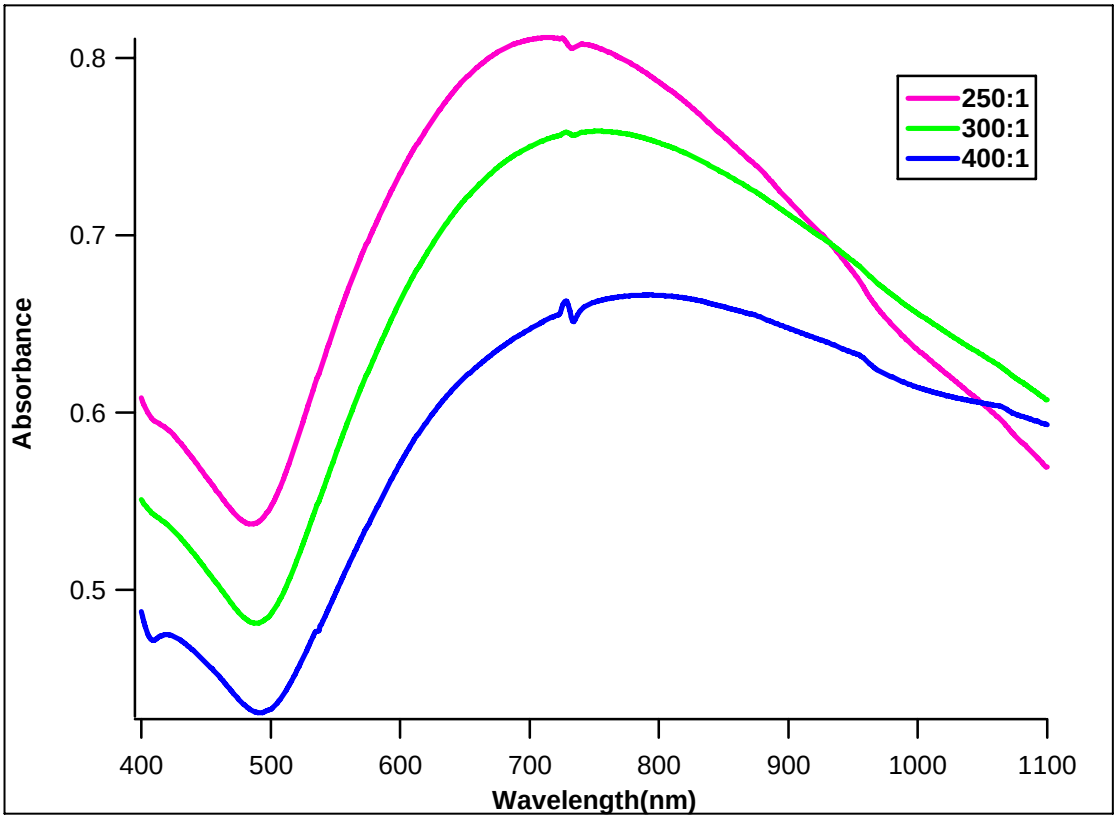

Figure 2.6: UV-vis spectra of gold nanoshells corresponding to the ratios - 250:1, 300:1, and 400:1

CHAPTER 3: SYNTHESIS AND CHARACTERIZATION OF TWO LAYERED HYBRID CORE GOLD NANOSHELLS

3.1 Synthesis of PNIPAM-Siloxane Hybrid Core Particles

In the presented work, two types of novel gold nanoshells were synthesized. The first is a two component material composed of a PNIPAM-Siloxane microgel coated with a layer of gold. The core hybrid particles were synthesized using a precipitation polymerization technique [24, 50, 51]. In this method N-isopropylacrylamide was copolymerized with 3-trimethoxysilylpropyl methacrylate (MPS) using potassium persulfate as the reaction initiator. The polymerization was done in the presence of N, methylenebisacrylamide (MBA) to create a cross-linked polymeric network containing siloxane groups [51]. This method is common in literature and has been used frequently to produce spherical, thermally responsive polymeric particles.

3.1.1 Experimental

- Materials: N-isopropylacrylamide (NIPAM) was purchased from TCI America, purified and re-crystallized in our lab. N, N, methylenebisacrylamide (MBA 98%) and potassium persulfate (KPS 99%) were purchased from Sigma Aldrich. 3-trimethoxysiylpropylmethacrylate (MPS 98%) was purchased from Acros Organics.
- Synthesis of Microgels: Using a 300mL round-bottom flask, 200mL of deionized water was degassed, by bubbling with N_2, for 1hour. Then, 1g of re-crystallized

NIPAM and 50mg of MBA, which is 5% of the monomer concentration, was added and bubbling continued for an additional 1hour at 75^{o}C. Separately, 20mg of KPS, which is 2% of the monomer concentration, was bubbled in 10mL of water at room temperature for 1hour. Once the monomer mixture was degassed and heated, the KPS solution was added to initiate the reaction. Two hours after adding the initiator, 240uL of the co-monomer, MPS, was added and the polymerization continued for an additional 2hours. The total reaction time was 6 hours. The microgel solution is cleaned in water using centrifugation. The particles were centrifuged at 6500rpm three to five times and between each centrifugation they were redispersed in deionized water. After the final water wash the microgels were redispersed in 50mL of water and stored at room temperature until use.

- Characterization Techniques: Dynamic light scattering (DLS) readings were taken using a Malvern Zetasizer Nano series instrument. The measurements were used to determine the size of the PNIPAM-siloxane core particles. Also, the microgels were imaged using transmission electron microscopy or TEM on a FEI Morgagni 268D model. DLS samples were prepared by dispersing 20uL of sample solution into 1mL of deionized water. This was done in a 2.5mL polystyrene cuvette. The cuvette was slightly shaken to ensure the dispersion of the nanoshells. TEM sample preparation involved dispersing 20uL of microgel solution in 1mL of deionized water and drying a few microliters of this solution on a formvar copper grid.

3.1.2 Results and Discussion

Thermally responsive PNIPAM-siloxane microgels were successfully synthesized using precipitation polymerization of NIPAM and MPS. An increase in co-monomer MPS can cause a decrease in thermal response and in some cases it has been noted in literature that the addition of large amounts of co-monomer (~40% of the monomer concentration) will produce microgels coated with a thin outer layer that show very little thermal response, if any [51]. Figure 3.1 shows the DLS trend graph for PNIPAM-siloxane microgels synthesized as per the procedure described in the experimental section above. The trend graph confirms the temperature dependent size response of the core microgel particles at temperatures between 40^{o}C and 20^{o}C. It displays that at high temperatures, above the volume phase transition temperature of cross-linked particles, 32^{o}C, the particle diameter is small around 225nm. This is due to the collapse of the polymer matrix and expulsion of water. For lower temperatures, below 32^{o}C, the matrix swells with water creating an increase in particle's diameter to ~300nm. A gradual diameter increase can be seen as the temperature of the particle solution decreases. TEM images in figure 3.2, show spherically shaped particles that are uniform in size.

3.2 Gold Seeding Using DP and LBL and Shell Growth

Nanoshells were grown on hybrid core particles that were seeded using the layer by layer technique (LBL) and the deposition precipitation method (DP). In the LBL process gold nanoparticles were synthesized through the reduction of hydrogen tetrachloroaurate (III) with a basic solution of NaOH [6, 13, 25, 52, 53]. For the DP method, synthesizing an additional gold nanoparticle solution was not necessary. Instead

the gold was directly precipitated onto the surface of the core particle [7, 16, 26, 30]. Gold seeded hybrid cores were first attempted using deposition precipitation. This technique was chosen because it diminishes the need to synthesize a separate gold nanoparticle solution and also because it was proven, in chapter 2, to be successful in synthesizing traditional silica core gold nanoshells. Because the attachment of small nanoparticles, ~2nm, to the microgel core was difficult to achieve using the DP technique, the LBL method was adopted. Using the LBL method under the right parameters produced uniformed gold decorated PNIPAM-siloxane hybrid particles. The shells were grown around the hybrid cores at different thicknesses to determine which exhibited the best optical properties, while maintaining the thermal responsiveness of the core.

3.2.1 Experimental

- Materials: Ammonium hydroxide (28-30%), chloroauric acid ($HAuCl_4 \cdot 3H_2O$ 99.9%), and tetrakis (hydroxymethyl) phosphonium chloride (THPC 80%) were purchased from Sigma Aldrich. Potassium carbonate and sodium hydroxide were purchased from Fischer Scientific. Sodium borohydride and sodium citrate were purchased from Acros Organics.
- Synthesis of Gold Nanoparticles**:** 2.54mM solution of $HAuCl_4$ was made by diluting 715uL of a 25mM gold solution in 6.5mL of water. The stock solution was kept in the dark at room temperature until used. A 1.2mM stock solution of THPC was made by dispersing 20uL of 80% THPC in 95mL of water. This solution was refrigerated when not in use. 1M NaOH stock solution was made by

dissolving NaOH salt in an aliquot of water. After preparing each stock solution gold nanoparticles were synthesized by dispersing 1.2mL of 1M NaOH and 4mL of THPC in 180mL of water. The solution was mixed continuously for 5-7minutes. 6.75mL of 2.54mM $HAuCl_4$ was added in a single injection, quickly, using an electronic pipette. Particles were refrigerated in an amber glass bottle until used.

- One-step Gold Seeding (DP Process): In the DP process the gold nanoparticles are precipitated in the presence of the core particles under slightly basic conditions. The pH of 10mL of 6.35mM $HAuCl_4$ was adjusted to approximately 8 through the slow addition of 0.1M NaOH. 1mL of hybrid core particles was mixed overnight in 2mL of NH_4OH. Through centrifugation most of the excess ammonium hydroxide solution is removed and the particles were dispersed in water. The particle solution was then added to the basic gold chloride solution and the mixture was vigorously stirred at 65^{o}C for 15 minutes. The solution was cooled to room temperature for 1hr. To remove any un-attached gold nanoparticles the solution was centrifuged at 1000rpm 3 times for 30 minutes each. The cleaned particles were dispersed in water and stored at room temperature.
- LBL Gold Seeding: The LBL method required the separate synthesis of gold nanoparticles described previously in this section. For this procedure, 3mL of hybrid microgels were mixed overnight in 6mL of NH_4OH. The ammonium hydroxide was then removed using centrifugation and the particles are redispersed in 4mL of water. 1.5mL of the ammonium soaked aqueous polymer solution was then incubated, at room temperature, with 10mL of freshly prepared gold

nanoparticles in a 20mL scintillation vial overnight. Centrifugation was used to separate any unattached gold nanoparticles and the seeded hybrid particles were redispersed in water.

- Gold Shell Growth: Gold seeded core particles, prepared using the LBL procedure, were used in the shell formation step. A gold precursor solution commonly called K-Gold is needed to grow the gold shell. It consists of, 1.5mL of 25mM $HAuCl_4$ mixed in 100mL of water for 1-2 minutes. 60mg of potassium carbonate was added to adjust the pH to approximately 10.1. The solution was mixed overnight in an amber glass bottle and the pH was taken after 24 hours of mixing. 10mM of sodium citrate was used as a capping agent. It was synthesized by dissolving an aliquot of sodium citrate salt in water. A strong reducing agent, 6.6mM sodium borohydride, was used to add additional gold onto the seeded hybrid core particle. This reagent was made by adding an aliquot of $NaBH_4$ to ice cold water. The reducing solution was kept in the freezer when not in use. Several core to shell ratios were synthesized for each, the amount of core particle solution was kept constant and the K-Gold amount was varied. The experiment described here is a 500:1, K-gold to core seed, ratio. 100uL of gold seeded hybrid core particle solution was dispersed in 50mL of K-Gold for 2-4 minutes. 2.5mL of 10mM sodium citrate was added to the core particle-K-gold solution and mixed for 2 minutes. 5mL of cold 6.6mM sodium borohydride was added in 250uL increments with 20 seconds between each addition. The solution was centrifuged and washed repeatedly in water to remove any un-reacted gold nanoparticles and finally dispersed in water.

- Characterization Techniques: FEI Morgagni 268D transmission electron microscopy was used to image each material described in this section, the DP seeded cores, LBL seeded cores, and the complete shell particles. Samples were prepared by drying ~20 microliters of diluted nanoshell solution onto a copper formvar grid. Jasco Spectrophotometer model V-530 was used to determine the position of the absorption band of the gold nanoparticles and the gold nanoshells at various shell thicknesses.

3.2.2 Results and Discussion

Reduction of gold chloride solution has been proven to be a good method for synthesizing nanosize gold particles capable of absorbing light in the visible region of the electromagnetic spectrum. Here, gold nanoparticles were synthesized using a simple reduction method. The formation of gold nanoparticles could be identified visually by a change is solution color from clear to brown. To determine the size of these particles, DLS was utilized. The size distribution graph, figure 3.3, shows particles with diameters of ~10nm or less, small particles are desired when seeding particles for nanoshell growth. Surface plasmon resonance for small gold nanoparticles is commonly seen around 520nm [1]. The optical absorption of the nanoparticles synthesized here was analyzed using UV-vis spectroscopy, shown in figure 3.4. These particles exhibit an absorption peak in the visible region at a wavelength of 518nm, typical for gold nanoparticles less than 20nm in size.

Gold nanoparticle seeding of polymeric microgels using deposition precipitation produced large clustered gold particles. TEM images, figure 3.5, display core particles

with a minimal amount of small uniformed gold nanoparticles attached. Many of the smaller gold nanoparticles found in the sample were unattached from the core particles. Much of the gold actually attached to a core consisted of large clusters of various sizes and shapes. Successfully creating nanoshells requires the gold seeds to be very small, ~2nm, and uniformed in size and shape. To accomplish this goal the seeding technique was switched from DP to LBL. The main stipulation when using the LBL technique is to seed hybrid core particles with freshly prepared gold nanoparticles. Over time gold nanoparticles will begin to aggregate in solution, this is indicated by a color change of the solution from brown to pale purple or darker depending on the size of the aggregates. Figure 3.6 shows the UV-vis spectra of freshly prepared gold nanoparticles compared to those that have been aged. A red shift is seen in the aged particles indicating an increase in particle size. For this reason, gold nanoparticles are stored at temperatures below 4^{o}C, but despite proper storage aggregation may still occur. If gold nanoparticles that are extremely aged (~weeks) are used for seeding, large gold clusters similar to those observed when using DP process, will attach to the core surface. Demonstrated in figure 3.7 are hybrid core particles seeded with aged gold nanoparticles compared with those seeded with freshly prepared nanoparticles. For the latter it is clear that the gold nanoparticle density is high and the particles are uniformed in shape and size, between 2-4nm.

Nanoshell growth is greatly dependent on the rate in which the reducing agent works. Sodium borohydride is a strong reducing agent, adding it in small increments is a way of controlling how fast the gold reduction happens. Using a capping agent is also helpful in reducing the speed of this process. Adding the reducing agent too quickly it

will result in the production of very thick nanoshells with optical properties similar to those of gold nanoparticles. TEM images, figure 3.8, were taken at different intervals of shell growth with a final ratio of 500:1. A sample was taken after the addition of 7 (1.75Ml), 9 (2.25mL), 12 (3mL), 15 (3.75mL), and 20 (5mL) injections of $NaBH_4$. The corresponding UV-vis spectra are shown in figure 3.9. From TEM it is obvious that increasing K-gold amount increases the amount of gold coating the core particle. UV spectra show that as the shell grows a red shift is seen but once a complete shell is formed a blue shift is observed. Figure 3.10 displays UV-vis spectra taken of a 500:1 core to shell ratio at various temperatures, ranging from room temperature to 55^{o}C. These graphs were used to determine if the collapse and swelling of the core particle played a role in the optical properties. It can be seen in these spectra that heating causes a slight red shift to occur and as the sample cools a blue shift is seen.

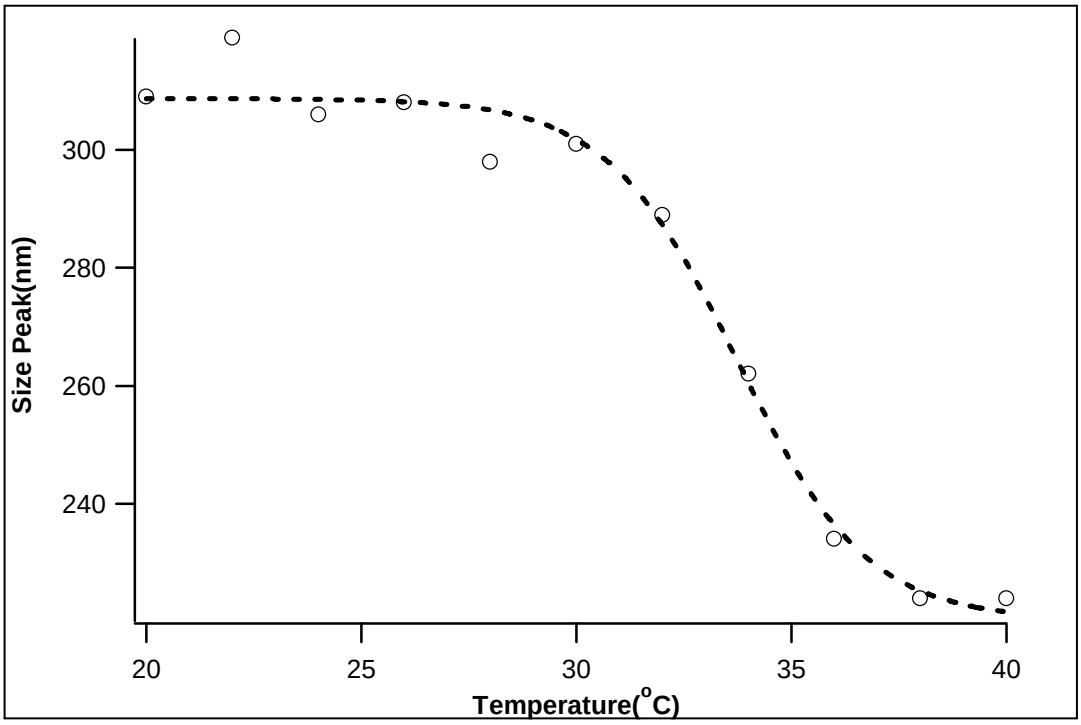

Figure 3.1: Variation of the hydrodynamic diameter of PNIPAM-siloxane hybrid particles as a function of temperature. The dashed line is drawn to guide the eye.

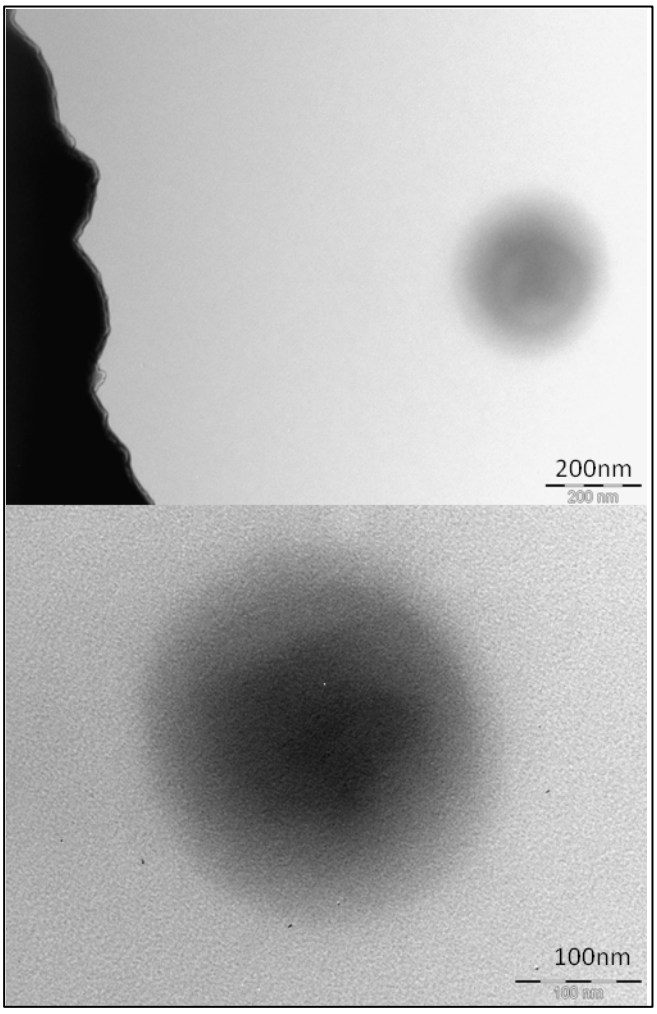

Figure 3.2: TEM images of PNIPAM-siloxane hybrid cores.

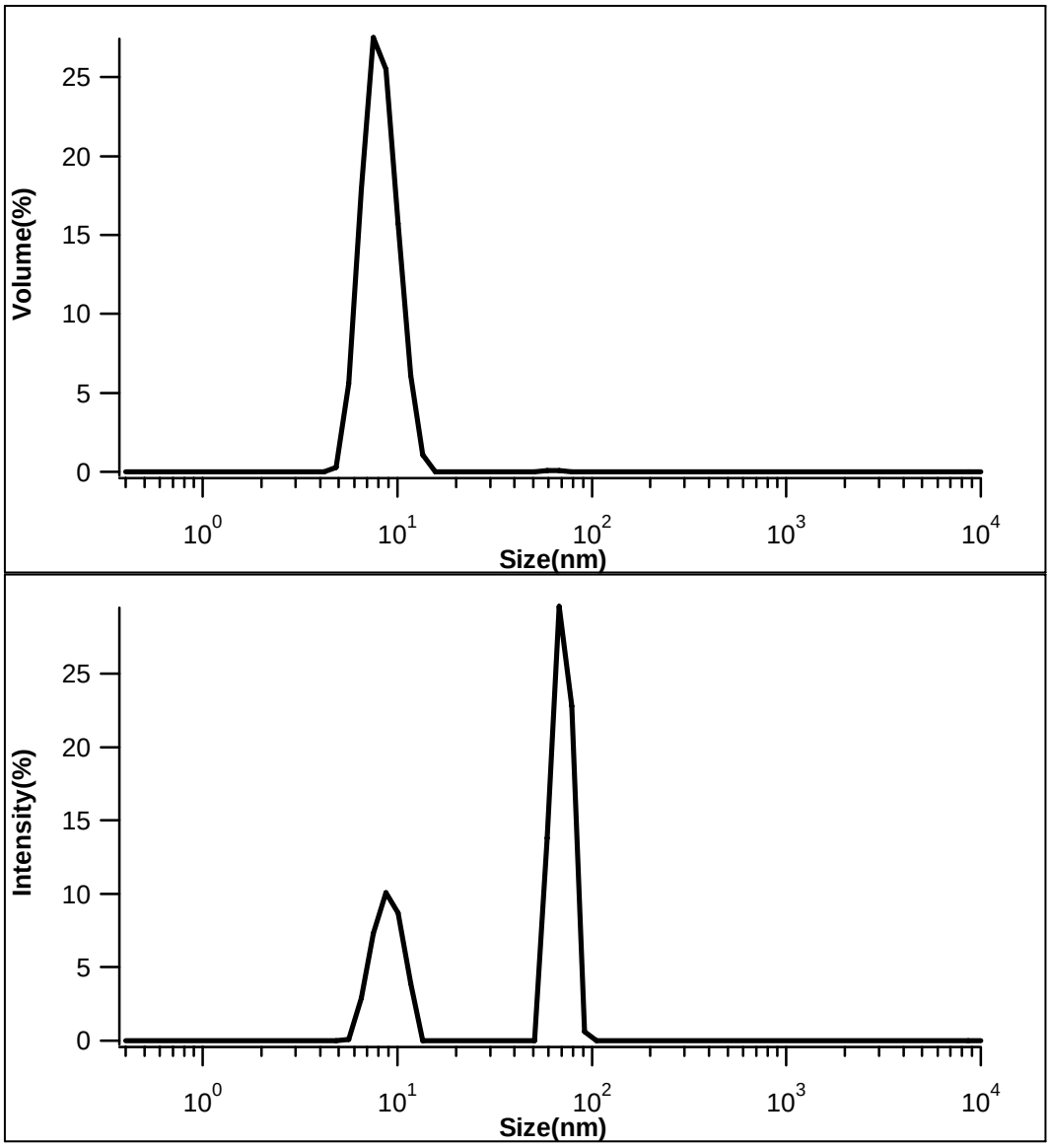

Figure 3.3: DLS size distribution plots for gold nanoparticles shown as volume scattering (top) and intensity scattering (bottom).

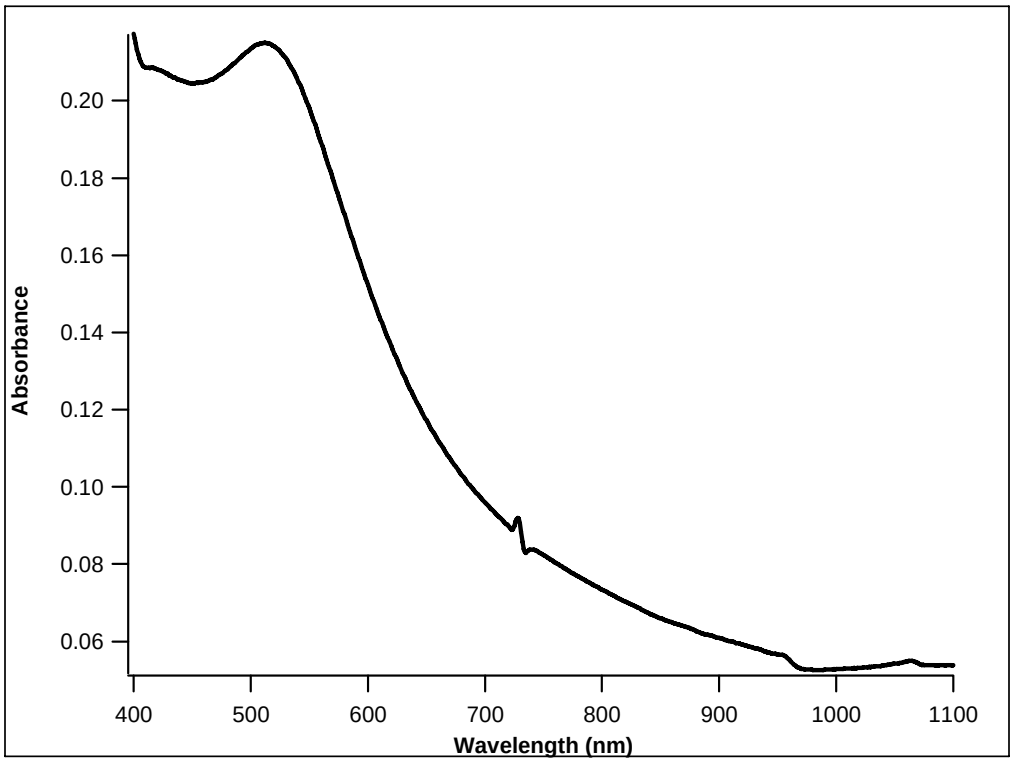

Figure 3.4: UV-vis spectrum of freshly prepared gold nanoparticles.

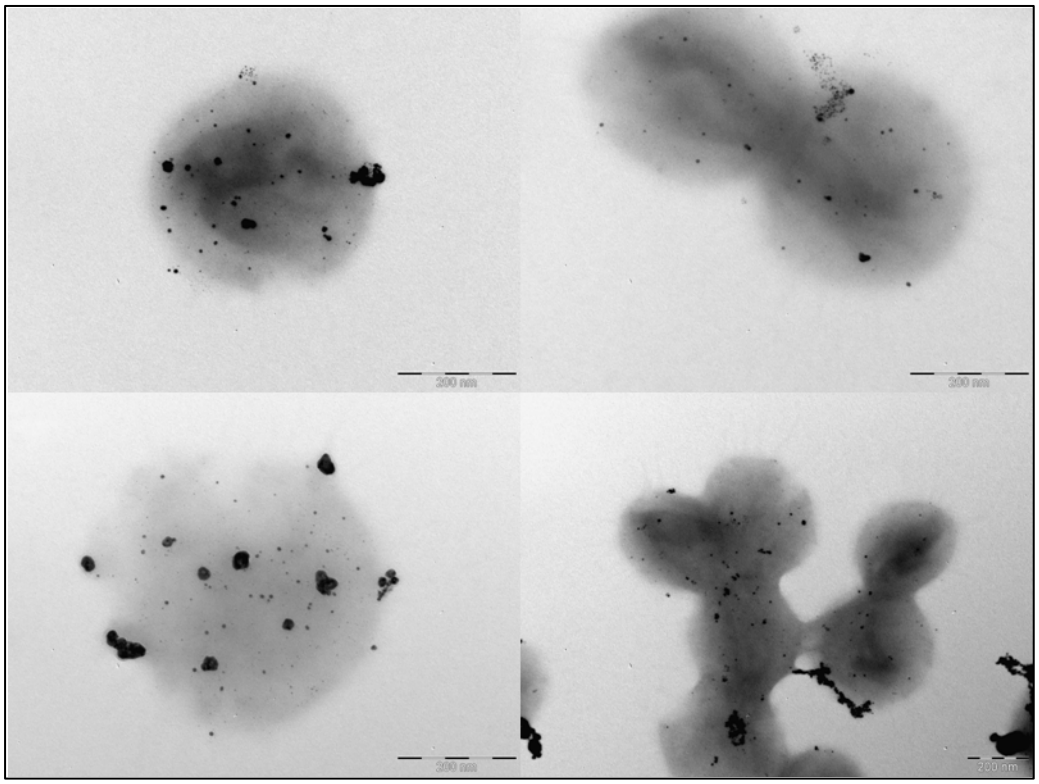

Figure 3.5: TEM images of PNIPAM-siloxane hybrid particle gold seeded with the DP method. All scale bars are 200nm.

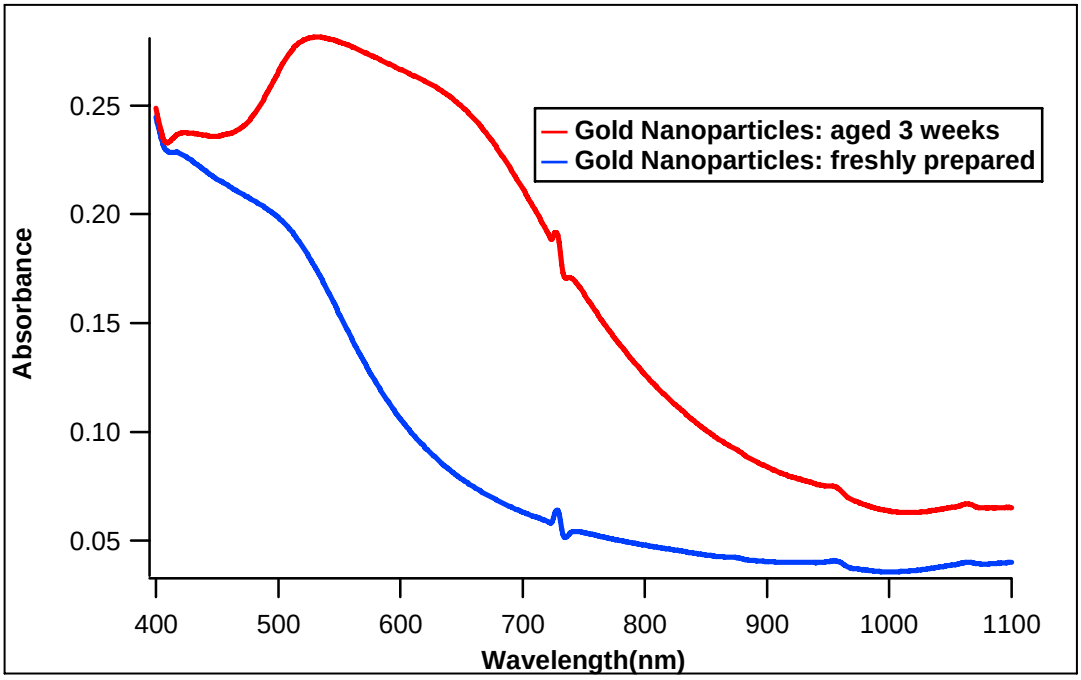

Figure 3.6: UV-vis spectra of fresh gold nanoparticles vs. aged gold nanoparticles.

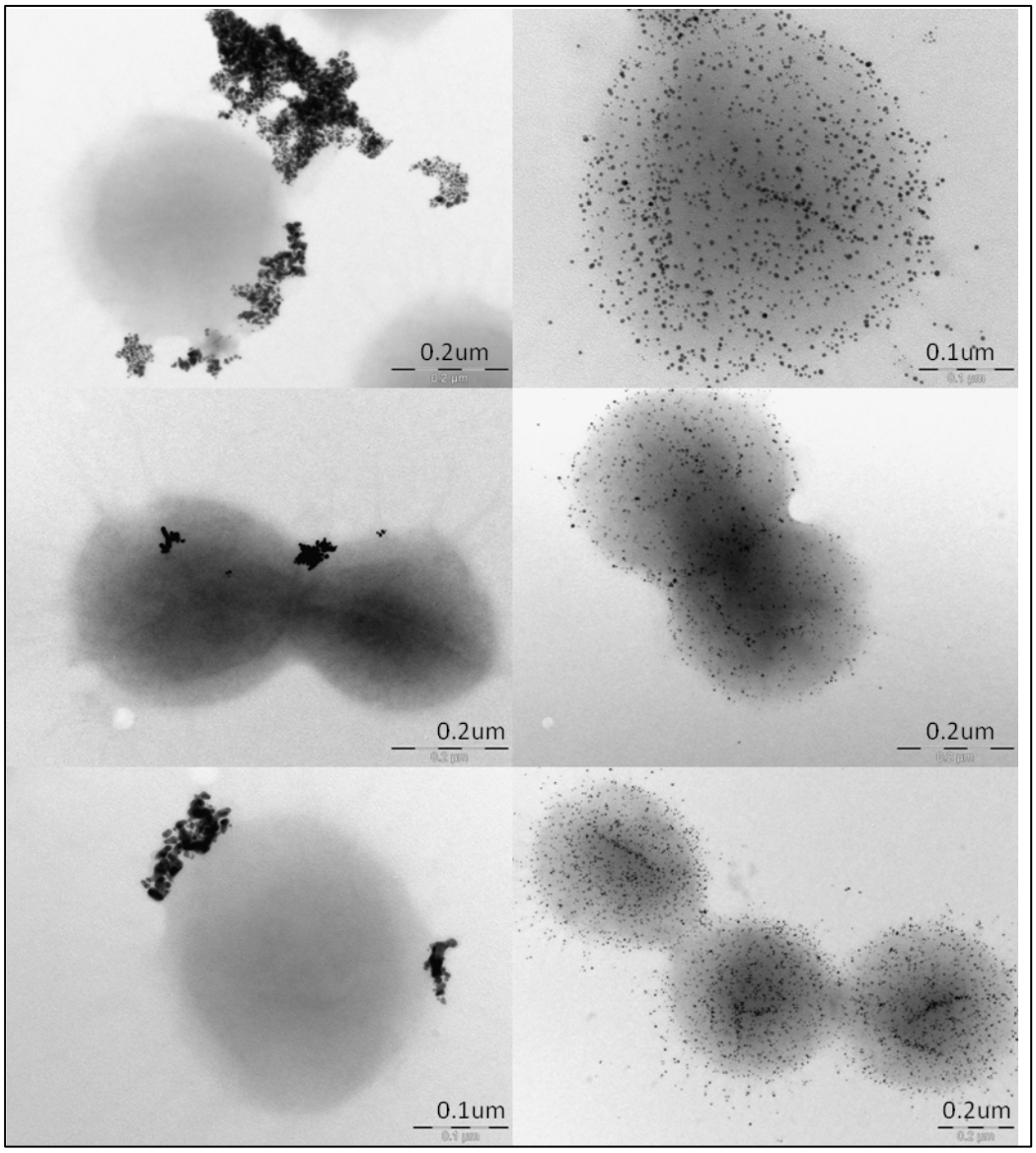

Figure 3.7: TEM images of PNIPAM-siloxane hybrid particles seeded using aged gold nanoparticles (left) and freshly prepared gold nanoparticles (right).

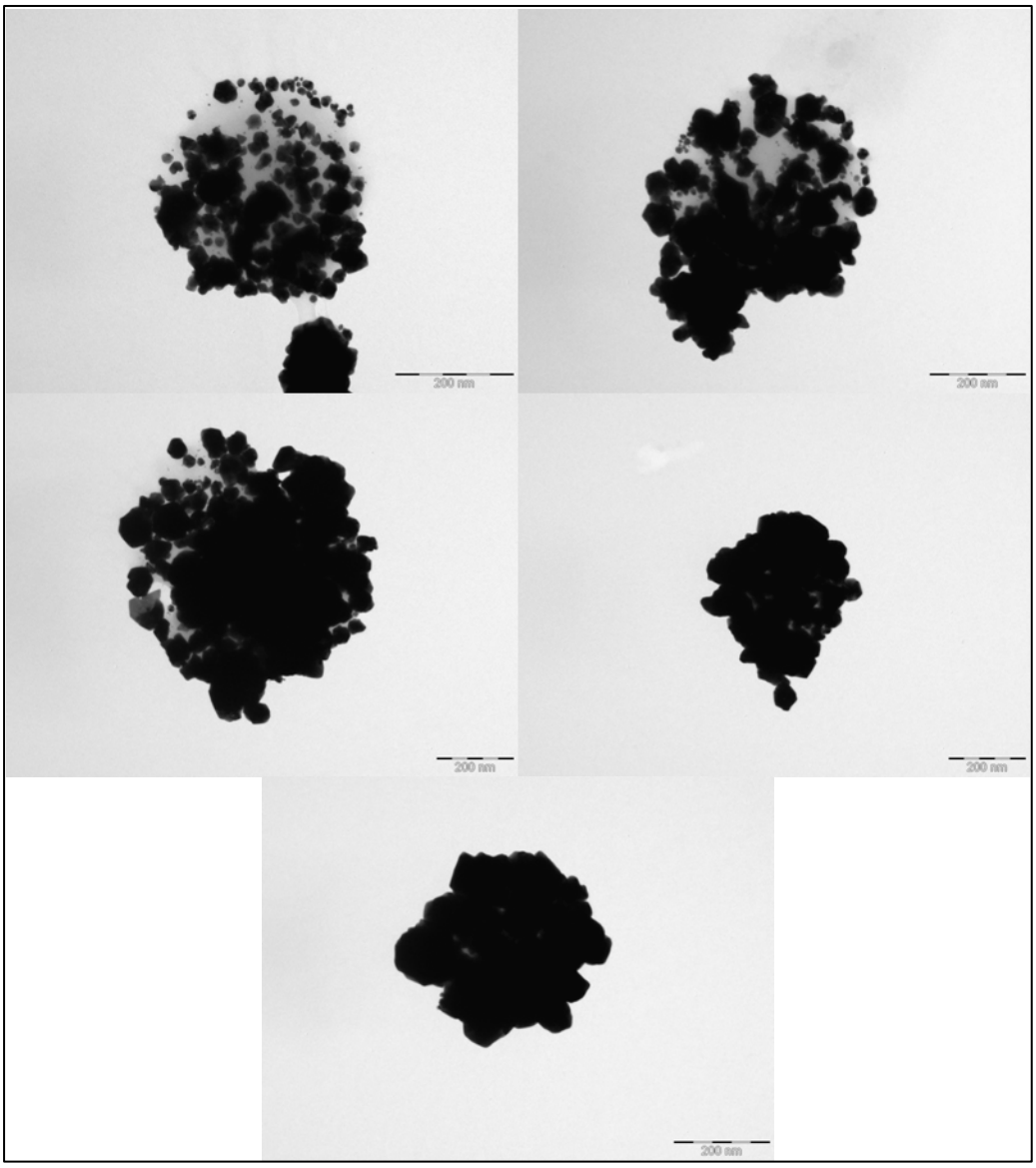

Figure 3.8: TEM of PNIPAM-siloxane hybrid gold nanoshells (50:1) at different intervals of the shell growth: 7 injections (top left), 9 injections (top right), 12 injections (middle left), 15 injections (middle right), 20 injections (bottom). All scale bars are 200nm.

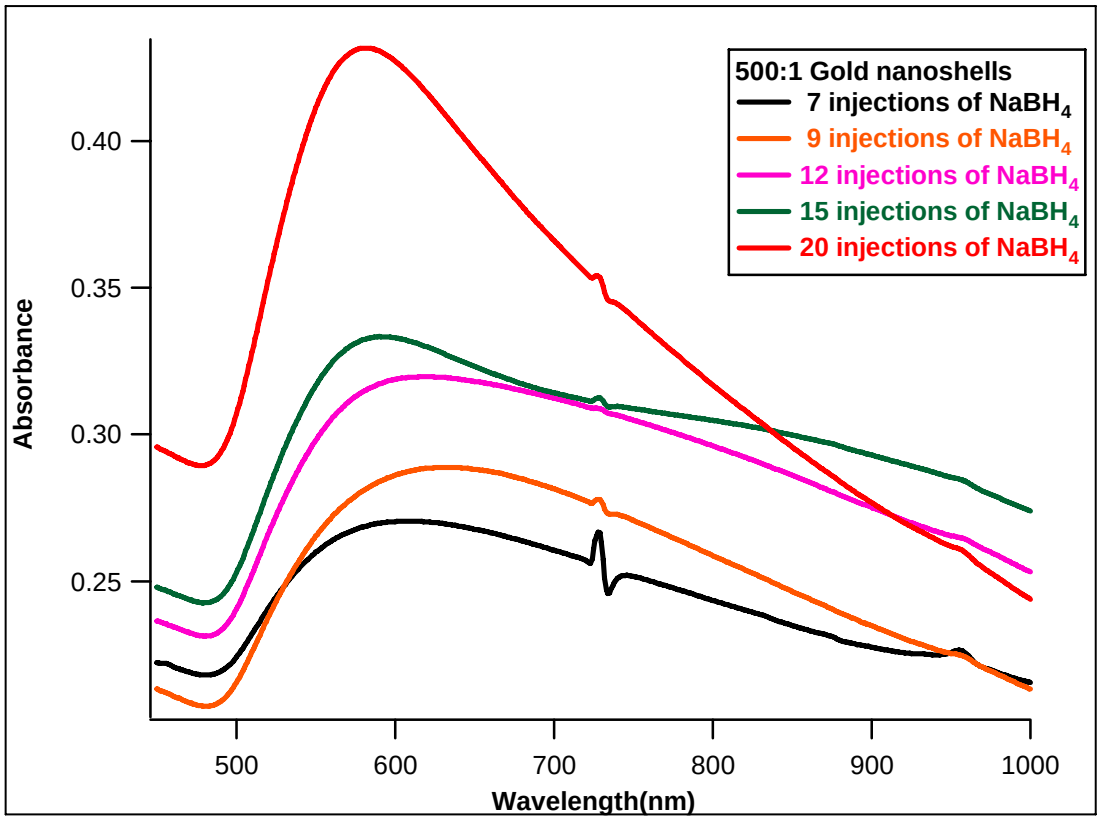

Figure 3.9: UV-vis spectra of PNIPAM-siloxane gold nanoshells at various intervals of shell growth as indicated in the legend.

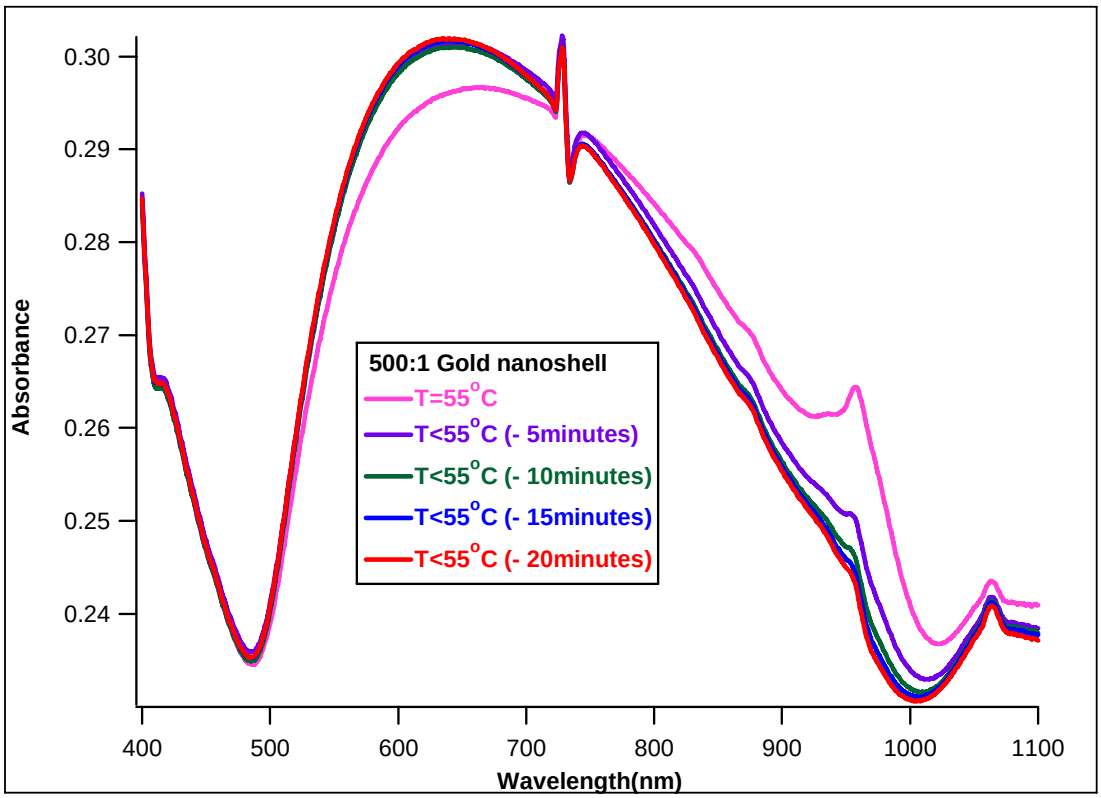

Figure 3.10: UV-vis spectra of PNIPAM-siloxane particles in solution as it cools from an initial T=55°C in 5 minute increments.

CHAPTER 4: SYNTHESIS AND CHARACTERIZATION OF THREE LAYERED SILICA CORE GOLD NANOSHELLS

4.1 Synthesis and Functionalization of Stöber Silica

Similar to core particles described in chapter 2, silica particles discussed here were synthesized using the well known Stöber method. As explained earlier, the Stöber method consists of two steps, first hydrolysis of ethoxy groups followed by the condensation of silicon hydroxide groups of tetraethylorthosilicate. Parameters of this reaction are fairly simple to control, and are easily manipulated to achieve particles of a desired size and morphology. The silica particles prepared here were later coated with a layer of poly N-isopropylacrylamide (PNIPAM). To encourage polymerization around its surface, silica was functionalized directly after synthesis using 3-methacryloxypropyltrimethoxysilane (MPS). MPS provides the silica surface with terminal vinyl groups, or carbon-carbon double bonds, that break to copolymerize with oligomers of NIPAM. A schematic of this is displayed in figure 4.1.

4.1.1 Experimental

- Materials**:** Ammonia hydroxide (28-30%) was purchased from Sigma Aldrich, ethanol was purchased from Pharmaco-AAPER & Commercial Alcohols, Deionized water was purified using Easypure UV water system, and both tetraethyl orthsilicate (TEOS 98%) and 3-trimethoxysilypropylmethacrylate (MPS 98%) were purchased from Acros Organics.

- Synthesis of Stöber Silica: In a 350mL round bottom flask, 30mL of water and 11mL of ammonia hydroxide were dispersed in 200mL of ethanol. The solution was allowed to mix vigorously for 30 minutes in a 70^{o}C oil bath. At that point, 16mL of TEOS was added and the reaction continued for 1 hour. For functionalization purposes, 50mL of the solution was kept in its original medium and the remainder was centrifuged and washed repeatedly in water to remove the ethanol residue.
- MPS Functionalization of Stöber Silica: In the same 350mL round bottom flask used for silica synthesis, 50mL of freshly prepared silica particles were functionalized in its original medium using MPS. 6mL of MPS was added to the 50mL solution and the solution was mixed vigorously overnight at room temperature. The mixture was then heated to 80^{o}C for 1 hour to promote covalent bonding. The product was then centrifuged and washed in water to separate out any un-reacted MPS and finally dispersed in fresh deionized water.
- Characterization techniques: Nicolet Magna IR Spectrophotometer (FTIR) was used to detect the presence of MPS on the surface of the silica particles surface. Samples were prepared by pelletizing a powder mixture containing sample particles and potassium bromide (KBr). Dynamic light scattering measurements were done using a Malvern Zetasizer Nano Series. The measurements were used to determine the size distribution of the silica particles. These samples were prepared by simply dispersing 20uL of the aqueous particles solution in 1mL of deionized water, within a 2.5mL polystyrene cuvette. TEM samples taken using a FEI Morgagni 268D were used to image the particles before and after

functionalization. Samples were prepared by drying ~20uL of sample solution on a copper formvar grid.

4.1.2 Results and Discussion

Bare silica particles and MPS functionalized silica particles were compared using FTIR spectrum, shown in figure 4.2. Similar to amine functionalized silica discussed in chapter 2, the IR spectra for MPS functionalized silica particles did not show any significant peak difference when compared to bare silica particles. Bare and MPS functionalized silica particles were imaged using TEM shown in figure 4.3. When compared to the bare silica, MPS silica particles were very similar in appearance. Although, the presence of MPS cannot be determined through IR absorption or TEM imaging characterization techniques, the successful formation of polymer coated silica, discussed later in this chapter, led us to conclude that terminal double bonds were present on the surface of the silica particles. Size distribution of bare Stöber silica was determined by DLS. The distribution graphs illustrated in figure 4.4 display the hydrodynamic diameter of silica in water to be ~170nm.

4.2 Polymerization of NIPAM in the Presence of Stöber Silica

As discussed in chapter one silica particles are capable of promoting polymerization of a monomer around its surface through the use of modifiers, preferably vinyl groups (-C=C). The use of MPS helps to overcome the natural hydrophilic nature of silica particles which encourages the attachment of hydrophobic NIPAM oligomers to the silica surface. Small silica particles have more surface area than larger particles.

Using small cores, less than 200nm decreased the chance for pure microgels, without a silica core, to form. Here, PNIPAM coated silica particles were synthesized using 170nm sized MPS grafted silica particles, described in the previous section. Polymerization was done in the presence of functionalized silica particles using a precipitation polymerization technique. In this technique, MPS-silica particles interact with NIPAM oligomers through the use of an initiator. The initiator creates terminal radicals on the monomer ends by breaking its double bonds. These radicals then interact with the double bonds on the functionalized silica surface to break and copolymerize with the monomer [23].

4.2.1 Experimental

- Materials: N- isopropyl acrylamide (NIPAM) was purchased from TCI America, purified and re-crystallized in the lab. N, N`-methylenebisacrylamide (MBA 99%) and potassium persulfate were purchased from Sigma Aldrich.
- Silica Core NIPAM Polymerization: In a 100mL three-neck round bottom flask, 58mg of NIPAM and 4mg of MBA were mixed in 10mL of water. This monomer solution was bubbled in a 45^{o}C oil bath for one hour. Separately, 15mL of was warmed and degassed with nitrogen. This solution was added to the bubbled monomer solution to increase the final reaction volume to ~25mL and in the same step an aqueous MPS-silica solution was added. At this point the temperature is also increased from 45^{o}C to 70^{o}C while N_2 bubbling and purging continued for an additional hour. Independently, an initiator solution was prepared by dispersing 6mg of KPS in 2mL of water. The solution was degassed for 20 minutes, and added to the NIPAM solution to initiate the polymerization reaction. The

reactants were mixed in a N_2 atmosphere for 6 hours after the addition of the initiator solution. The particles were washed using water and centrifugation to remove any unattached monomer and cross-linker.

- Characterization Techniques: Nicolet Magna IR Spectrometer 860 (FTIR) was used to detect the presence of PNIPAM on the surface of silica particles. The thermal response and size distribution of PNIPAM-silica particles was determined by dynamic light scattering using a Malvern Zetasizer Nano Series, and a FEI Morgagni 268F transmission electron microscope was used to image the silica particles before and after polymerization.

4.2.2 Results and Discussion

Bare silica particles were compared to PNIPAM coated silica particles using FTIR, DLS, and TEM. In figure 4.5, the FTIR spectrum of PNIPAM-silica displays an intense peak around 1000cm^{-1} which indicates the presence of Si-O-Si groups. In this same spectrum hydrocarbon peaks between 2500 and 3000cm^{-1} are present as well as peaks that are typically seen in amide bearing materials, namely around 1650, 1550, and 1460cm^{-1}. When compared to the PNIPAM-silica, IR spectrum of bare silica only exhibits the Si-O-Si peak. DLS plots demonstrate a particle diameter increase after attachment of the polymer shell. The size distribution of silica and PNIPAM coated silica at 20^{o}C are presented in figure 4.6. The diameter of bare silica was measured to be around 170nm and this diameter increased to approximately 300nm for PNIPAM coated silica. Figure 4.7 displays the diameter in response to decrease in temperature from 40^{o}C to 20^{o}C of the PNIPAM-silica particles. At room temperature (~20^{o}C), PNIPAM-silica

particles possess a diameter of 345nm. This temperature is below the volume phase transition temperature of cross-linked NIPAM meaning that the polymer matrix is swollen with water. At 40^{o}C, above the volume phase transition temperature the polymer matrix is collapsed and the water is expelled this results in a smaller hydrodynamic diameter, ~ 250nm. TEM images in figure 4.8 compare bare silica particles to PNIPAM-silica particles. In these images the polymer layer in PNIPAM-silica can be distinguished from the core due to the difference in density of each material. Silica is denser than PNIPAM therefore the core of the particle appears darker than the less dense outer shell.

4.3 Gold Seeding and Shell Growth on PNIPAM Coated Silica

PNIPAM-SiO_2 particles were gold seeded by reducing gold salt solution in the presence of the polymeric core particles. Chloroauric acid was diffused into the polymer layers of the particles and reduced, which resulted in gold nanoparticles within the polymeric layers and around the surface of the PNIPAM-SiO2 cores. This process was done at room temperature or below to ensure the polymer matrix was expanded as much as possible, to increase the uptake of gold solution. Increasing the amount of gold solution in within or around to core particles increases the number of gold nanoparticle nucleating sites formed. The nanoshells were grown in using the same technique discussed in chapter two, with the exception that some samples were made using a different reducing agent. For this material sodium borohydride and formaldehyde were used as reducing agents to grow the metallic shell. Formaldehyde was chosen because it is a much weaker reducer compared to sodium borohydride making it easier to control the shell growth rate.

4.3.1 Experimental

- Materials: Chloroauric acid ($HAuCl_4 \cdot 3H_2O$ 99.9%), was purchased from Sigma Aldrich, potassium carbonate and sodium hydroxide were purchased from Fischer Scientific, and Sodium borohydride, sodium citrate, and formaldehyde (37%) were all purchased from Acros Organics.
- Gold Seeding PNIPAM-silica: In an 8mL scintillation vial, 1.88mL of 2.54mM HAuCl4 was mixed with 2mL of PNIPAM-SiO2 solution for 25 minutes. Separately, in a 50mL conical flask, 166uL of 1M NaOH and 550uL of THPC were vigorously mixed in 25mL of water at room temperature. Quickly, the gold-PNIPAM-SiO2 solution was added to the basic aqueous solution and the reduction reaction continued for 1 hour. The particles were then centrifuged and washed in water to remove any unattached gold nanoparticles. Several core to shell ratios were synthesized but for explanation purposes, the 500:1 K-gold to core particle solution is described for the sodium borohydride shell growth and a 50:1 ratio is detailed for the formaldehyde grown nanoshells.
- Shell Growth on PNIPAM-silica using $NaBH_4$: A K-Gold Solution consisting of 60mg of K_2CO_3 and 1.5mL of 25mM $HAuCl_4$ dissolved in 100mL of water was aged for two days in an amber glass vial. After one day the pH was measured to be 10.06. A 10mM sodium citrate solution was prepared by dissolving 40mg of citrate salt in 13.6mL of water. A reducing agent stock solution of 75mM sodium borohydride was prepared by dissolving 26mg of $NaBH_4$ powder in 9mL of water. The 6.6mM $NaBH_4$ solution needed for the reaction was diluted from the 75mM stock. In a 60mL glass bottle, 50mL of K-gold was heated to 50^{o}C for 5

minutes before adding 100uL of gold seeded PNIPAM-silica particles. The solution continued to mix vigorously for 10 minutes before 2.5mL of 10mM of sodium citrate was added. One minute after the addition of sodium citrate, 5mL of 6.6mM $NaBH_4$ was added in 20 increments of 250uL approximately 1 minute apart and the reaction continued for 15 minutes.

- Shell Growth on PNIPAM-silica using Formaldehyde: In a 20mL scintillation vial, 10mL of K-gold and 200uL of gold seeded PNIPAM-silica particle solution were mixed and heated to 55^{o}C for 10minutes. 25uL of formaldehyde was then added and the reduction reaction continued for 15 minutes.
- Characterization Techniques: Transmission electron microscopy, FEI Morgagni 268D model, was used to image gold seeded PNIPAM-silica and gold shell coated PNIPAM-silica. Samples were prepared by placing ~20uL of particle solution on a formvar copper grid and allowing the grid to dry under a visible lamp. A Jasco V-530 UV/Vis Spectrophotometer was used to take UV-vis spectrum of the complete nanoshell material. The spectra were used to determine the optical properties of the nanoshells at various shell thicknesses and temperatures.

4.3.2 Results and Discussion

TEM images and UV-vis spectra were used to determine the presence of the gold nanoshells at various synthesis stages. For gold seeded PNIPAM-silica, TEM images shown in figure 4.9, illustrate that gold nanoparticles between 2-6nm densely populate the polymeric matrices of the core particles. This particle size was ideal for creating

uniformed gold shells. TEM images shown in figure 4.10 are of 500:1 gold nanoshells grown using sodium borohydride. It can be seen from these images that the shells were incomplete and that there were large gold aggregates both attached to the core particles and free in the solution. TEM images of 250:1 gold nanoshells, also in figure 4.10, displayed core particles that were coated with more gold than that seen in nanoshells described above. The 250:1 particles were expected to have less gold than the 500:1 particles simply because the gold ratio was lower, therefore, it is assumed that the inconsistency in the shell formation is due to the excess aging (2 days) of the K-Gold solution used for the 500:1 gold nanoshells. Both the 500:1 and the 250:1 samples were prepared using the same procedure, except in the 250:1 the K-Gold solution was only aged for 1 day. These findings helped us to determine that the age of the K-Gold solution played a major role in the formation of the gold shell. Images taken of formaldehyde grown nanoshell, 50:1 and 20:1, are shown in figure 4.11. Both types of particles had rough and incomplete shells. Large gold aggregates were also seen in both samples, especially 50:1, presumably due to the increase in K-Gold. UV vis spectra were recorded at various temperatures for sodium borohydride (500:1), formaldehyde (50:1), and formaldehyde (20:1) grown gold nanoshells. For the 500:1 shells grown with $NaBH_4$ two sets of spectra were taken, the first was taken on the day of synthesis shown in figure 4.12, and the second was taken 4 days after synthesis, shown in figure 4.13. The spectra for 500:1 nanoshells grown using $NaBH_4$ display two absorption peaks, a main peak in the visible region around 600nm and a second in the near infrared region at approximately 960nm. The initial spectrum is taken at 45^oC directly after synthesis and the following 3 are taken approximately every 5 minutes as the sample cooled. The fifth

and sixth spectra were taken after 55 minutes and 3 hours of cooling, respectively. For those spectra taken 4 days posy-synthesis the sample was initially reheated to 55^{o}C and then allowed to cool. A spectrum was taken every 5 minutes for 15 minutes total. The overall collection of spectra, for figures 4.12 and 4.13, shows that as the temperature of the sample increase, the visible peak remains almost constant but the near infrared peak intensifies to absorb more irradiated light. The shift in peak intensity was reversible and when the sample temperature cooled the NIR peak declined in intensity. The main difference between the spectra taken on the day of synthesis and those taken after some time was that the intensity of the visible and NIR peaks in the latter were much less intense. The lack of intensity in the aged sample could be due to the aggregation of gold on the core particle surface or even the separation of these large clusters from the core particle. The nanoshells grown using formaldehyde offer slightly different optical properties, the properties for a 50:1 and a 20:1 ratio are displayed in the UV-vis spectra shown in figure 4.14 and 4.15, respectively. The absorption spectra for both the 50:1 and 20:1 ratios show a broad peak that spans from the visible region, 600nm well into the near infrared region, 1000nm. The broadness of this peak increased as the sample cooled to room temperature. For each ratio, the first spectrum was taken at 55^{o}C and at this temperature the peak is seen more in the visible region. Four additional spectra were taken in 5 minute intervals as the temperature of the sample decreased. Here, the peak broadened as the sample cooled. When a lower amount of formaldehyde, 20:1, was used the broadening of the peak as the sample cooled was much greater when compared to those synthesized using a larger formaldehyde ratio, 50:1. The visible region peak is believed to be a result of the collapse in the polymeric matrix. When the matrix was

collapsed the gold aggregates were closer together causing an optical absorption similar to that of gold nanoparticles. The broadening seen in the absorption peak as the sample cooled was presumably a result of the gold aggregates being forced apart due to the increase in the core particle diameter.

Based on the results presented in this chapter, PNIPAM coated silica particles were successfully synthesized and these hybrid core particles were able to be converted into three layered thermally responsive gold nanoshells with unique optical properties.

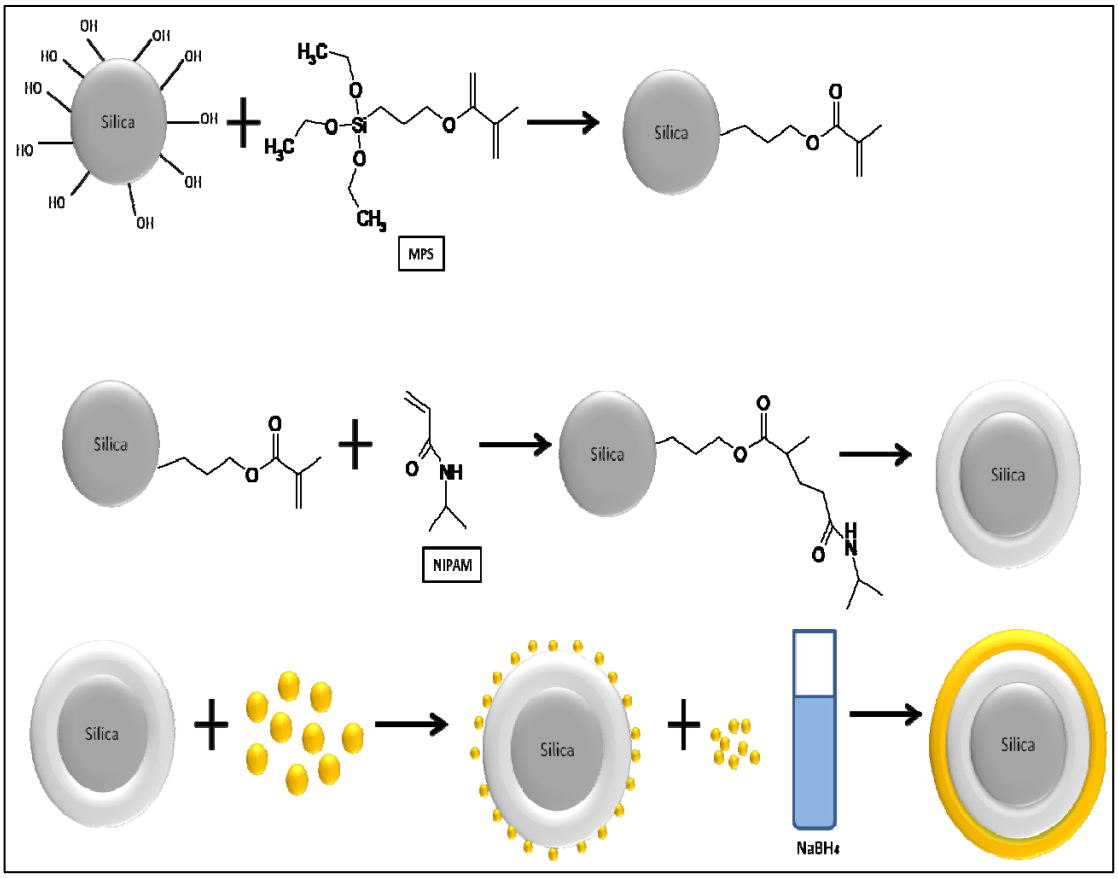

Figure 4.1: Schematic synthesis of three layered gold nanoshells.

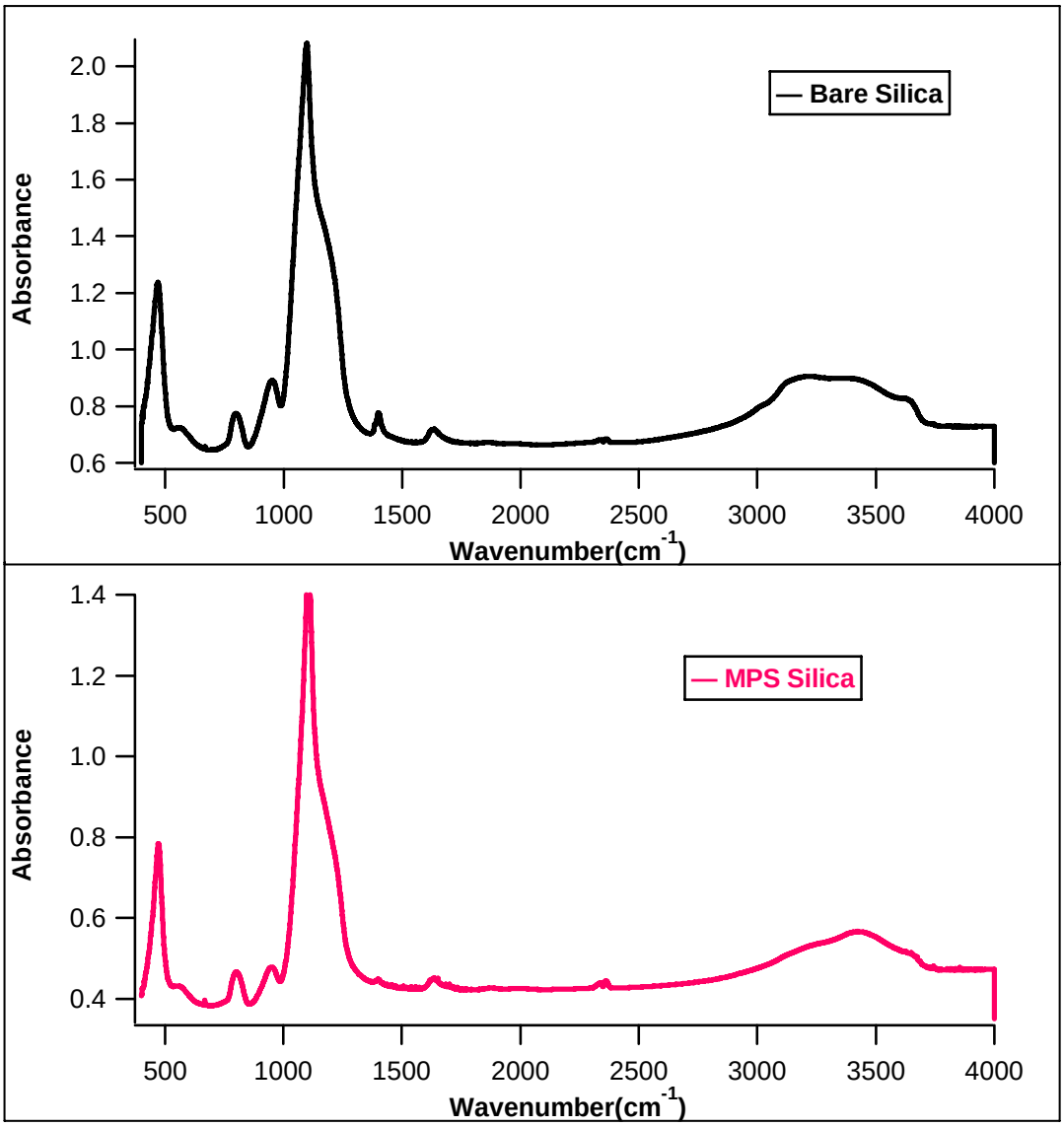

Figure 4.2: FTIR spectrum of bare silica particles (top) compared to MPS grafted silica particles (bottom).

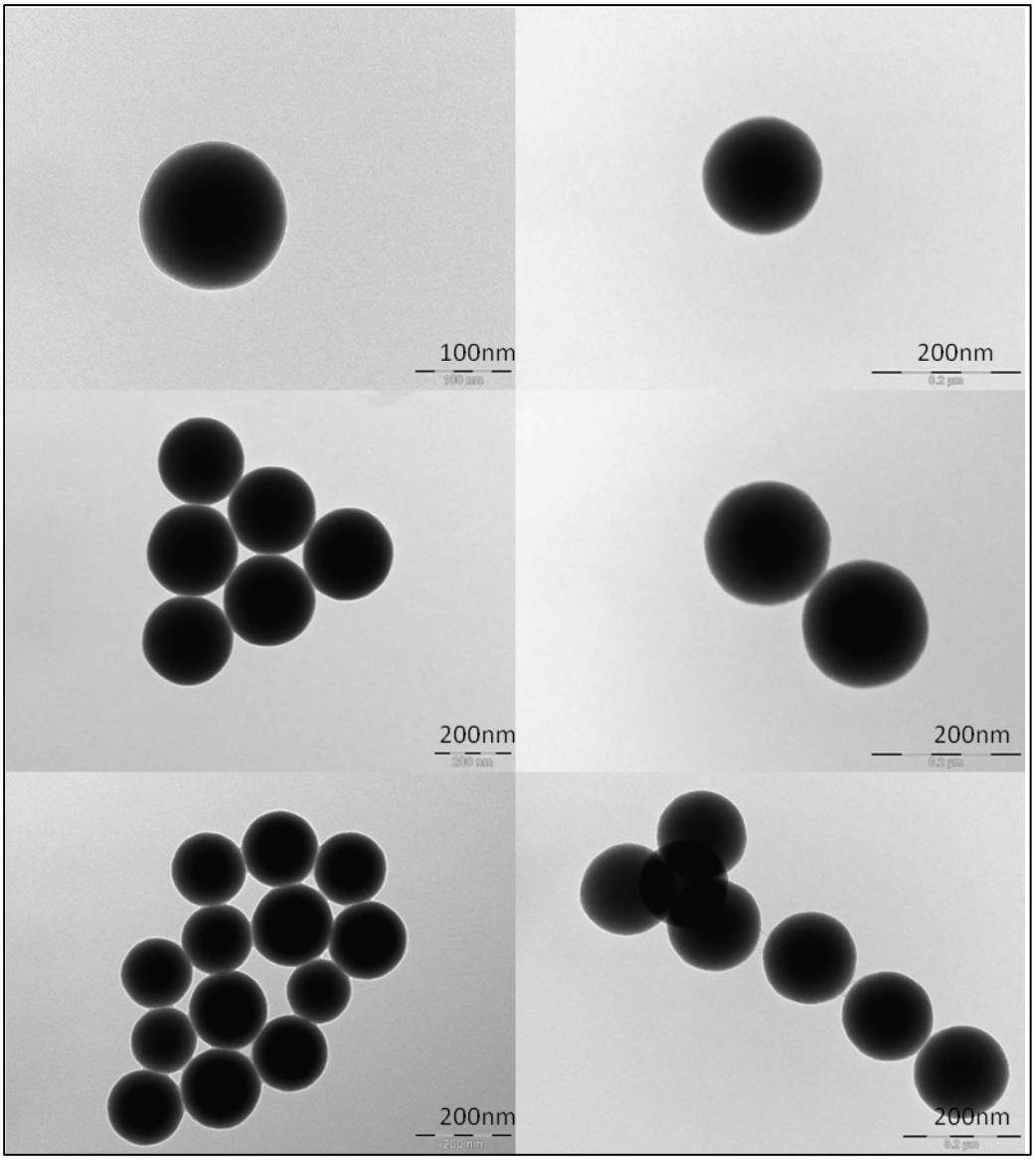

Figure 4.3: TEM images of bare silica particles (left column) compared to MPS grafted silica particles (right column).

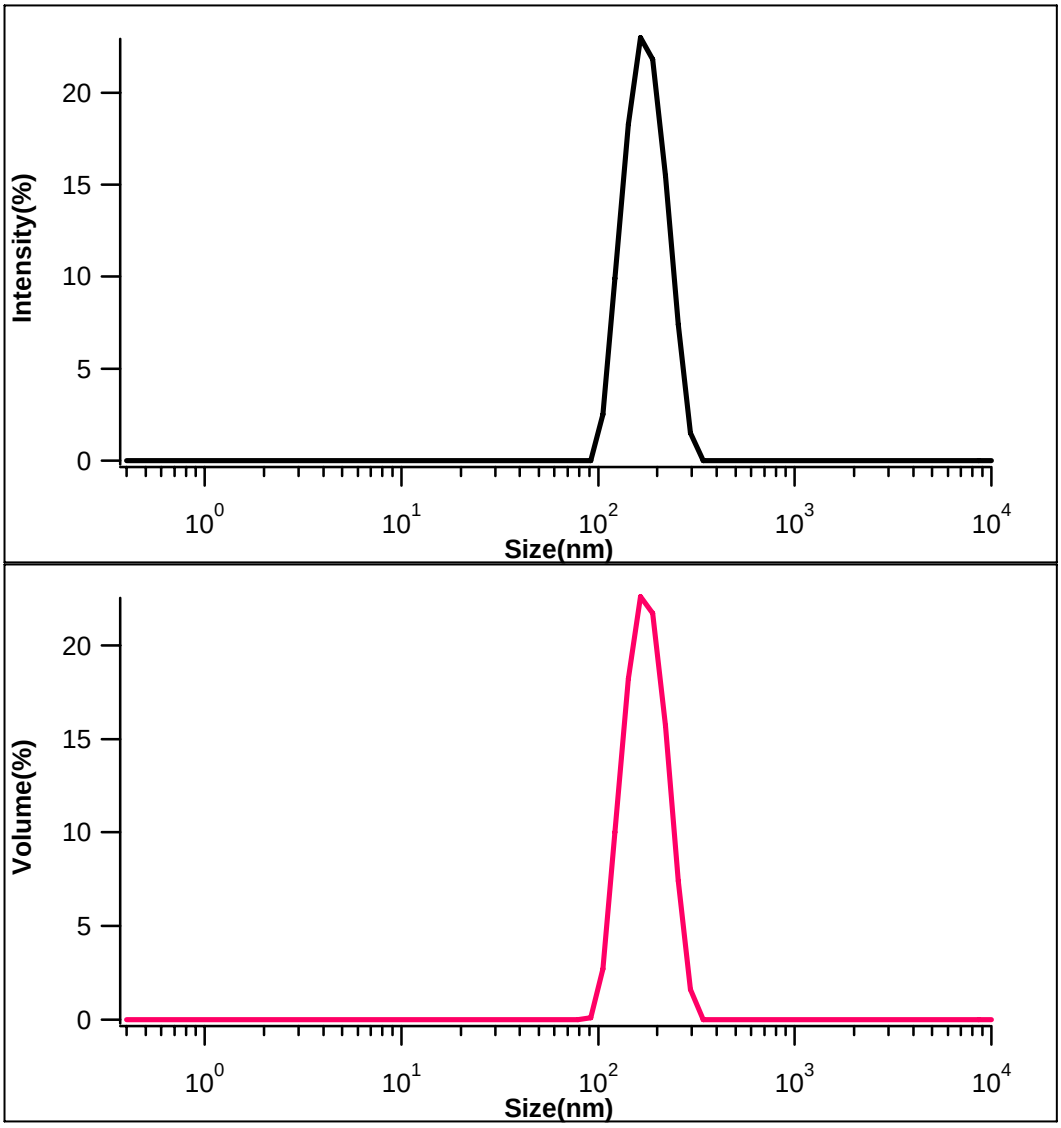

Figure 4.4: DLS measurements showing intensity scattering (top) and volume distribution (bottom) of bare silica particles.

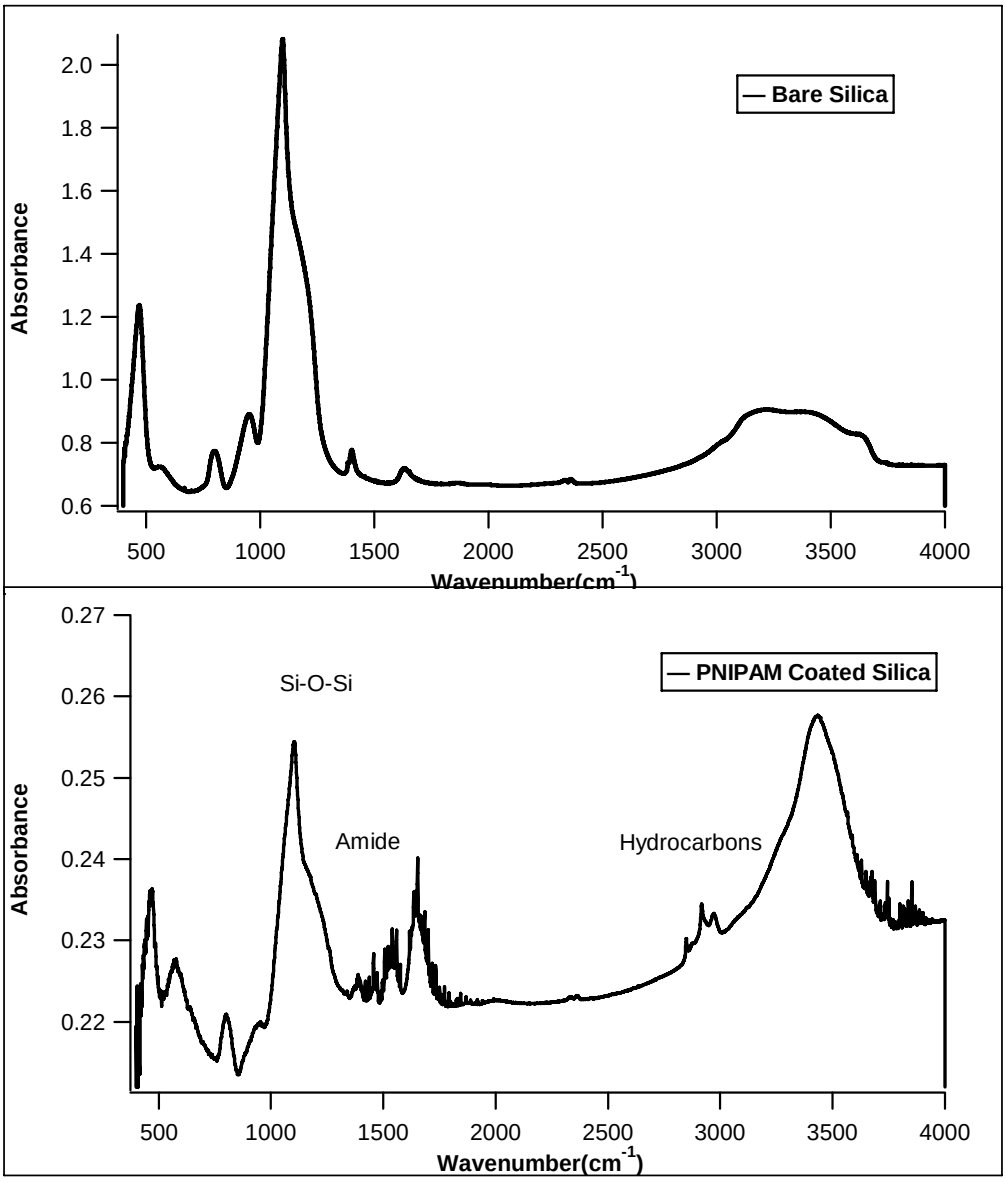

Figure 4.5: FTIR spectrum of bare silica particles (top) compared to PNIPAM coated silica particles (bottom).

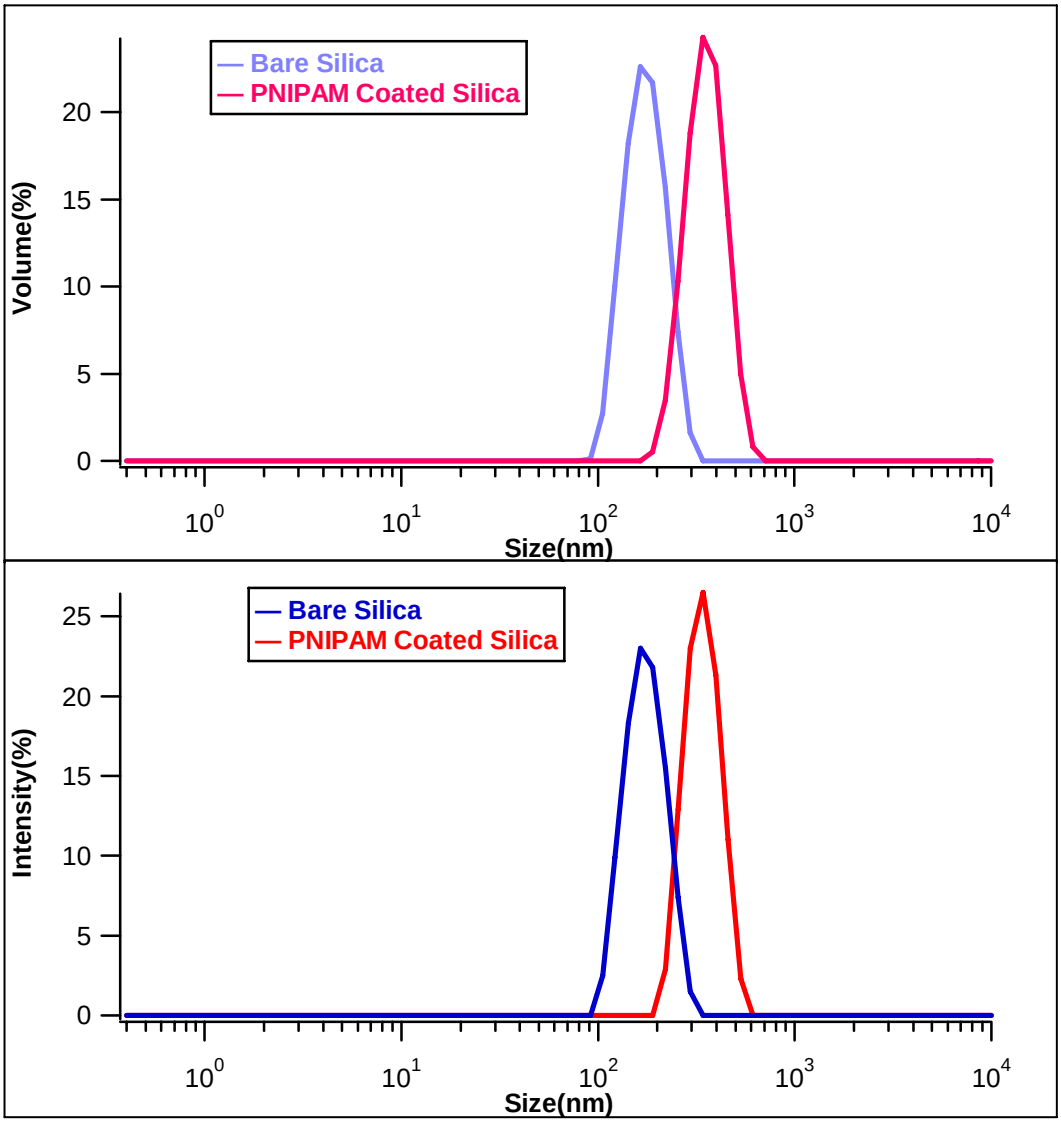

Figure 4.6: DLS distribution graph of blank silica compared to PNIPAM coated silica particles: intensity (top) and volume (bottom).

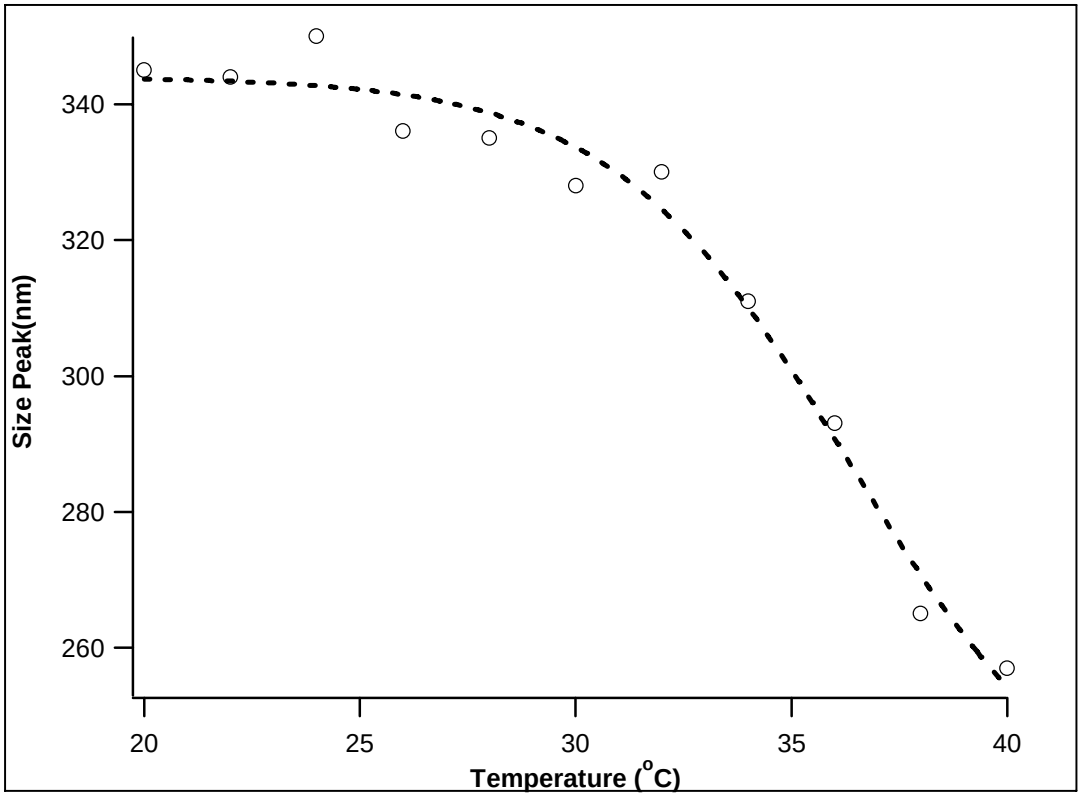

Figure 4.7: Variation of hydrodynamic diameter from DLS of PNIPAM coated silica particles as a function of temperature. The dashed line is drawn to guide the eye.

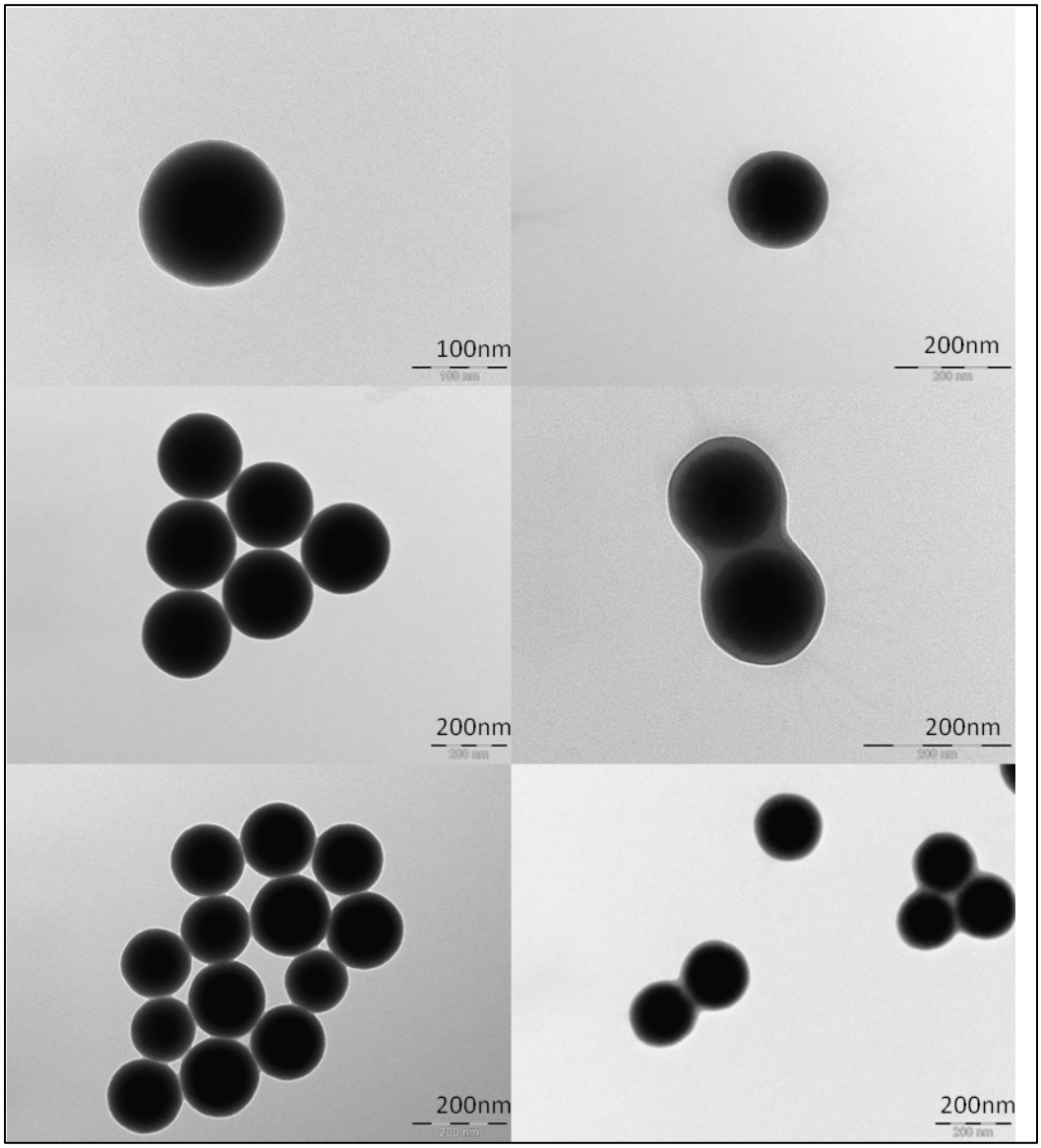

Figure 4.8: TEM images of bare silica particles (left) compared to PNIPAM coated silica particles (right)

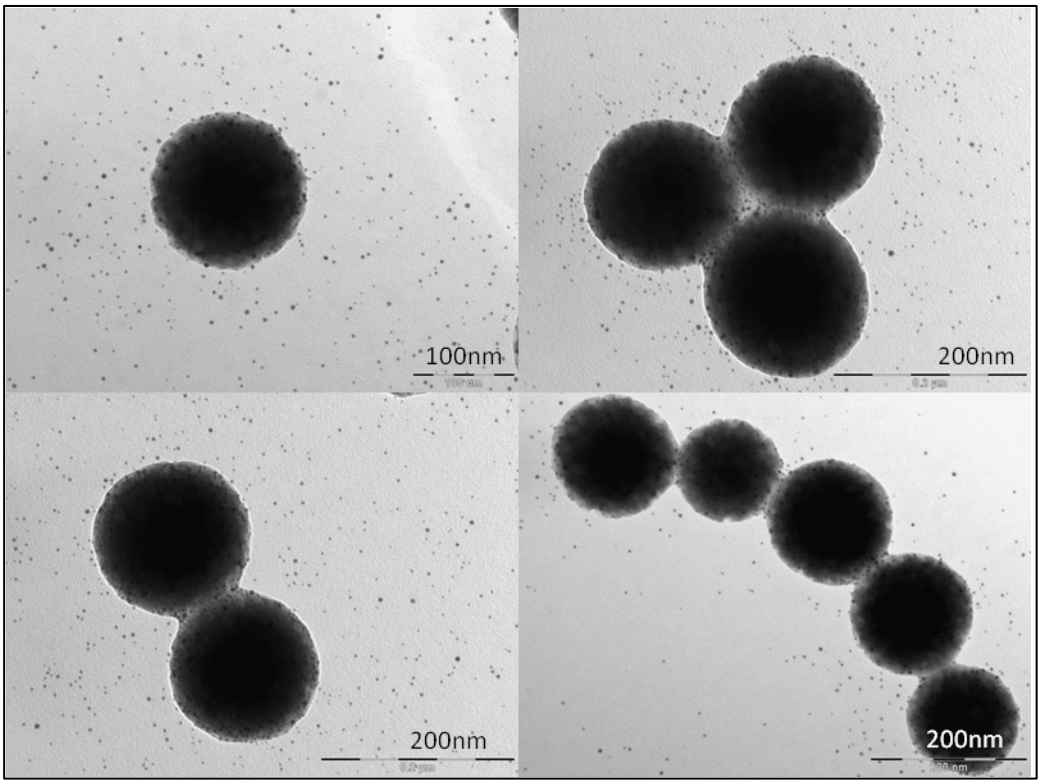

Figure 4.9: TEM images of gold seeded PNIPAM-silica particles

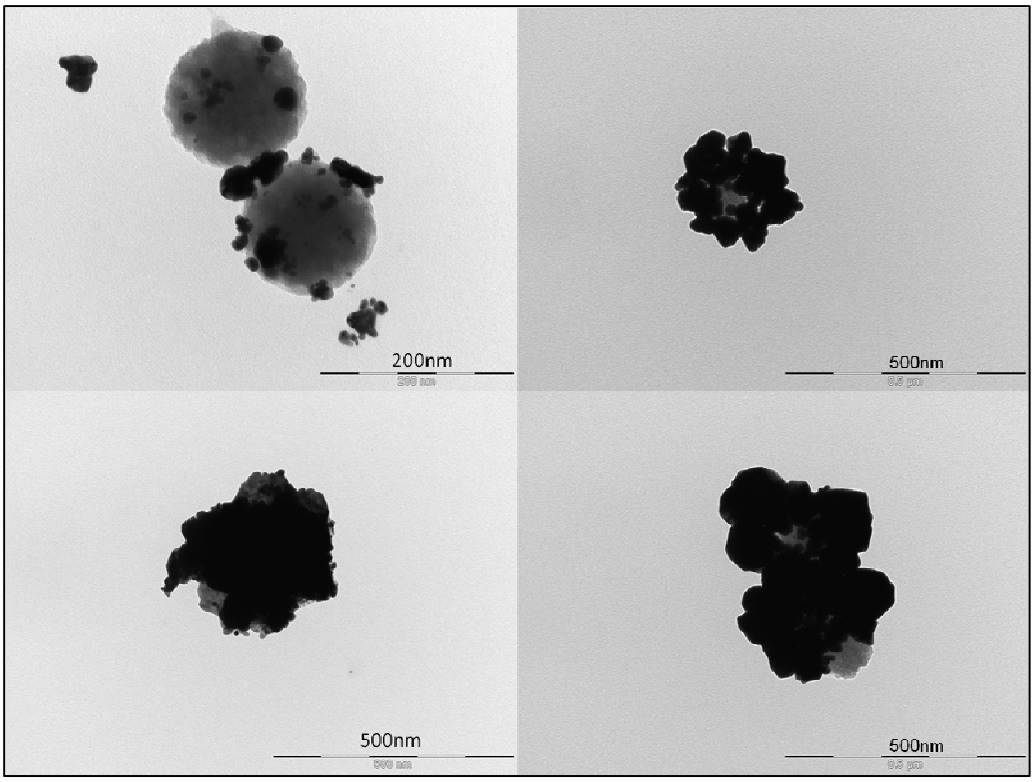

Figure 4.10: TEM images of nanoshells with K-Gold to seed ratio of 500:1 (left) and 250:1 (right) prepared using sodium borohydride route.

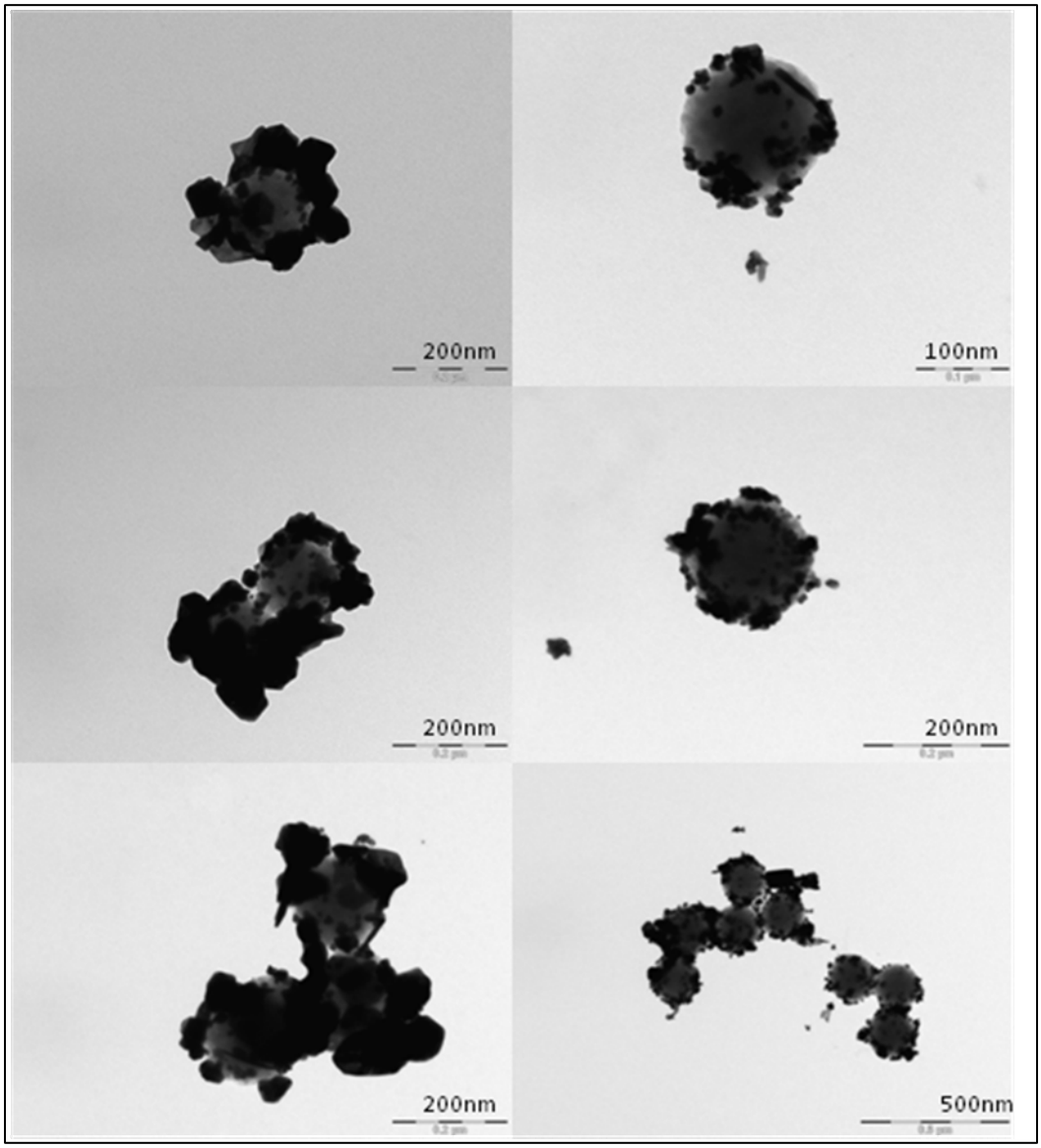

Figure 4.11: TEM images of nanoshells with K-Gold to seed ratio of 50:1 (left) and 20:1 (right) prepared using formaldehyde.

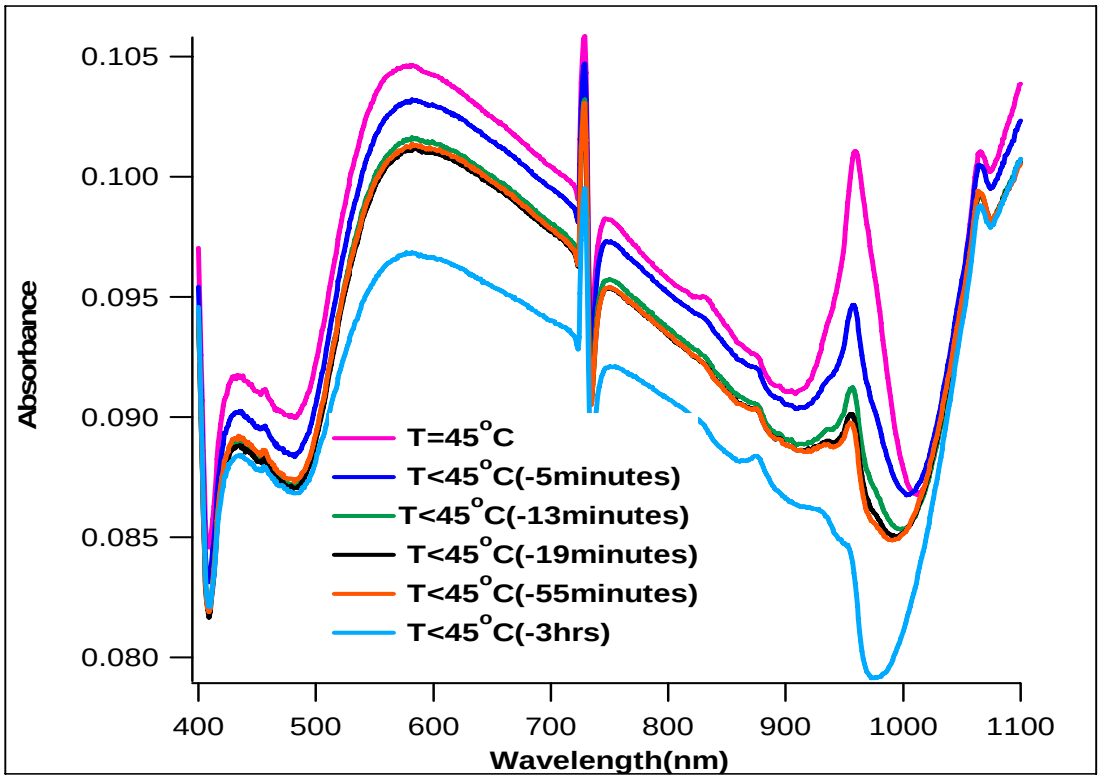

Figure 4.12: UV-vis spectra of 500:1 ratio nanoshells prepared using sodium borohydride. The spectra are measured as sample cooled from 45°C to room temperature.

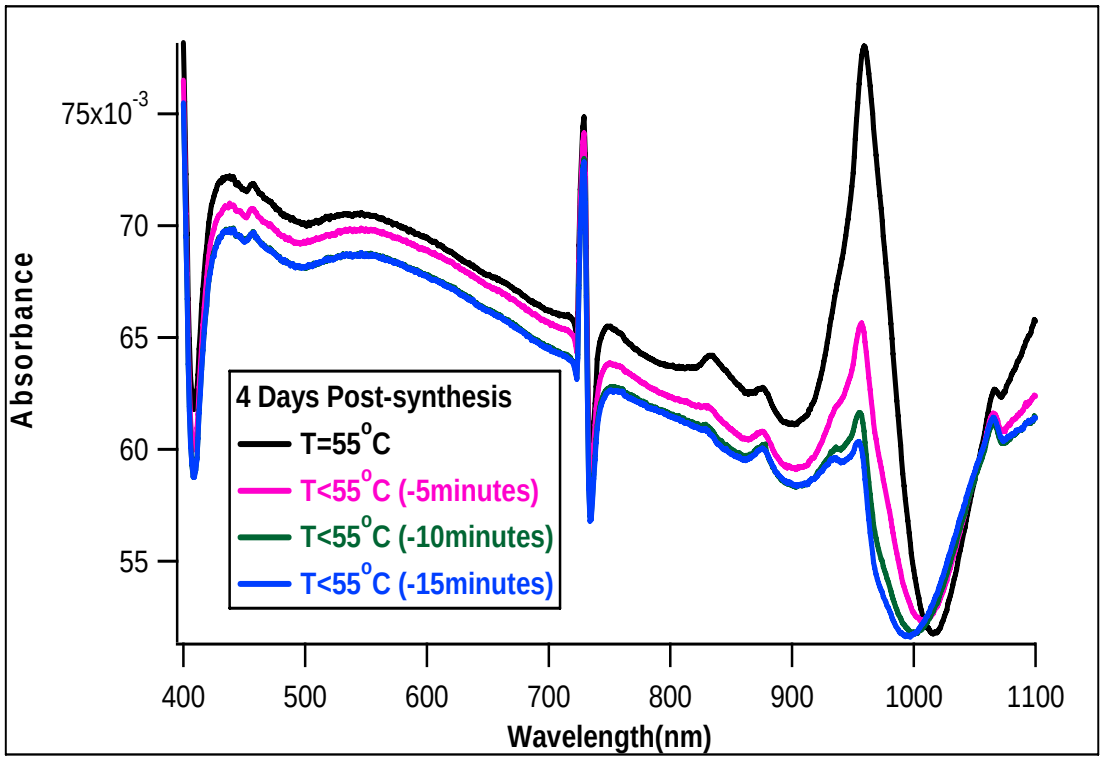

Figure 4.13: UV-vis spectra of 500:1 ratio nanoshells prepared using sodium borohydride. The spectra were taken 4 days after synthesis and are measured as sample cooled from 55°C to room temperature.

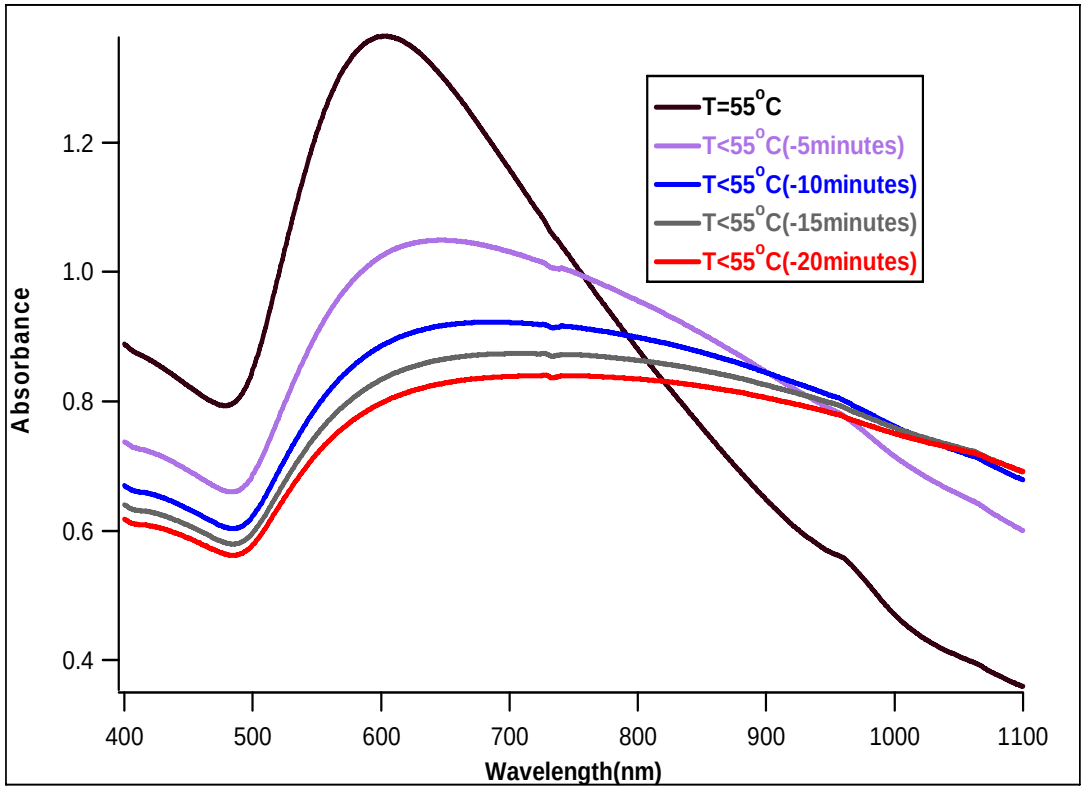

Figure 4.14: UV-vis spectra of 50:1 ratio nanoshells prepared using formaldehyde and taken every 5 minutes for 20 minutes total as sample cooled from 55°C.

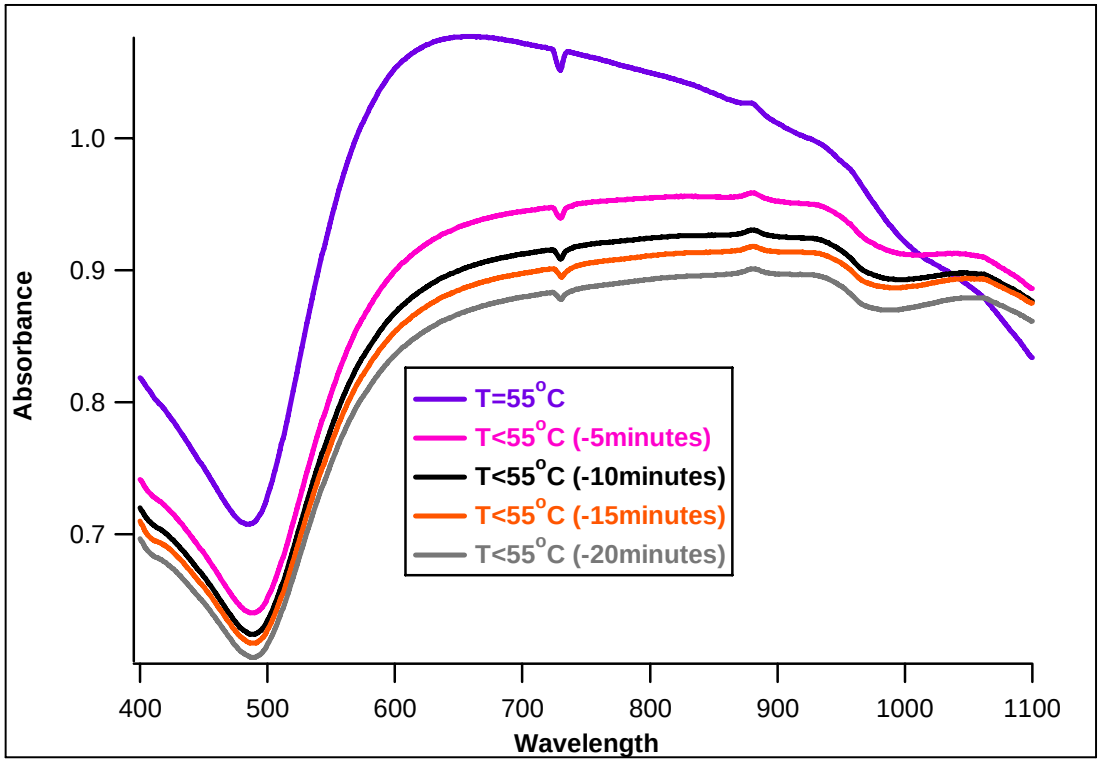

Figure 4.15: UV-vis spectra of 20:1 ratio nanoshells prepared using formaldehyde and taken every 5 minutes for 20 minutes total as sample cooled from 55°C.

CHAPTER 5: SUMMARY OF RESEARCH

In summary, the research in this thesis successfully developed two novel thermally responsive gold nanoshell materials. The novel nanoshells materials combined for the first time an inorganic and an organic component. Specifically, the first nanoshell is a two layered material constructed of a PNIPAM-siloxane hybrid core coated with an outer layer of gold. The second material consists of three layers, a silica core, PNIPAM middle layer, and an outer gold shell. Each of these materials was successfully synthesized using a layer by layer technique. By changing various parameters, such as temperature, concentration, pH, and reaction time, the core particle size, thermal response of the polymer layer, and the gold shell thickness can be controlled. Controlling each of these parameters is very important because they each play a key role in the optical properties exhibited by the material.

The two layered hybrid core nanoshells are described in chapter three. Results from this chapter confirm the synthesis of thermally responsive hybrid core particles. It was demonstrated using DLS that the hybrid microgels were free to collapse and swell with temperature change, prior to the addition of the gold shell. These particles, although less dense than traditional nanoshell cores, are capable of supporting a gold nanoshells on their surfaces. Based on UV-vis spectroscopy results the incorporation of a shell around the hybrid core did not hinder the thermal responsiveness of the particles. UV-vis also revealed that a change in particle diameter induced a slight red shift in the optical

absorption spectrum. Although optically responsive particles were synthesized TEM images displayed particles with incomplete and uneven shells. Further investigations are needed to determine the exact amount of gold solution and reducing agent needed to create particles with uniform shells of a desired thickness. It is assumed that creating uniform nanoshells will enhance the optical properties even further.

Chapter four details the synthesis and properties of three layered gold nanoshells. These particles consist of silica cores, as seen in traditional gold nanoshells, coated with PNIPAM, and lastly a layer of gold. Silica particles were incorporated because they are known in literature to produce stable gold nanoshells. The polymer coating was used to maintain the thermal responsiveness found in the hybrid core nanoshells detailed in chapter 3. Results from DLS revealed that the polymer middle layer is temperature responsive and there is no hindrance from the silica core particle. When compared to the hybrid core particles, described in chapter three the polymeric layer of the three component nanoshell was more thermally responsive presumably due to the lack of a co-monomer. Images taken using TEM demonstrate that many of the polymer coated silica particles contained two or more silica cores. TEM images taken of the gold nanoshells displayed incomplete shells and large gold aggregates attached to the core particles as well as freely dispersed within the sample. Finally, by utilizing UV-vis spectroscopy a thermally responsive NIR peak was clearly defined. Further research is needed to determine the optimum silica diameter to prevent the production of multi-core PNIPAM-silica particles. More studies are also needed to perfect the shape and uniformity of the gold nanoshell.

Incorporating organic components into this normally inorganic material was a novel contribution to the field of nanomaterials. Both materials presented here, the hybrid core and the PNIPAM-silica core gold nanoshells, exhibited unique thermal and optical properties, in solution. For both two and three layer gold nanoshells grown using a strong reducing agent, $NaBH_4$, we saw a NIR peak whose absorption intensified proportional to temperature increase. The absorption properties of these materials caused heat to dissipate from the particle surface and as a result the surrounding environment was heated. As the environmental temperature increased the particle absorbed more NIR light, this cyclic process created a continuous heating system, in solution. For three layer gold nanoshells grown using formaldehyde, a weaker reducing agent, we saw a different set of thermal and optical properties. Here, the absorbance band decreased and became broader as a result of a temperature decrease. This property could contribute to the potential development of novel nanomaterials with the ability to automatically discontinue absorption as the surroundingl temperature increases.

Solar conversion systems commonly exist as flat panels or as a coating dried on a linear surface therefore, in future work the formation of these novel gold nanoshells into monolayers on flat substrates will need to be studied. Also, determining how the confinement of these particles to a flat substrate will influence their thermal and optical properties will also need to be thoroughly investigated. By exploiting these properties new and more efficient solar conversion systems can potentially be developed.

REFERENCES

1. Yong, K.T., et al., *Synthesis and plasmonic properties of silver and gold nanoshells on polystyrene cores of different size and of gold-silver core-shell nanostructures.* Colloids and Surfaces a-Physicochemical and Engineering Aspects, 2006. 290(1-3): p. 89-105.

2. Kalele, S., et al., *Nanoshell particles: synthesis, properties and applications.* Current Science, 2006. 91(8): p. 1038-1052.

3. Jain, P.K., et al., *Noble Metals on the Nanoscale: Optical and Photothermal Properties and Some Applications in Imaging, Sensing, Biology, and Medicine.* Accounts of Chemical Research, 2008. 41(12): p. 1578-1586.

4. Cole, J.R. and N.J. Halas, *Optimized plasmonic nanoparticle distributions for solar spectrum harvesting.* Applied Physics Letters, 2006. 89(15): p. -.

5. Catherine J. Murphy, T.K.S., Anand M. Gole, Christoher J. Orendorff, Jinxin Gao, Linfeng Gou, Simona E. Hunyadi, and Tan Li, *Anisotropic Metal nanoparticles: Synthesis, Assembly, and Optical Applications.* Journal of Physical Chemistry B, 2005. 109: p. 13857-13870.

6. Pham, T., et al., *Preparation and characterization of gold nanoshells coated with self-assembled monolayers.* Langmuir, 2002. 18(12): p. 4915-4920.

7. James C.Y. Kah, n.P., Rachel C. Y. Wan, Jing Song, Timothy White, Subodh Mhaisalkar, Iman Ahmad, Colin Sheppard, Malini Olivo, *Synthesis of gold nanoshells based on the deosition-precipitation process.* Gold Bulletin, 2008. 41(1): p. 23-36.

8. Caruso, F., R.A. Caruso, and H. Mohwald, *Production of hollow microspheres from nanostructured composite particles.* Chemistry of Materials, 1999. 11(11): p. 3309-3314.

9. Caruso, F., et al., *Multilayer assemblies of silica-encapsulated gold nanoparticles on decomposable colloid templates.* Advanced Materials, 2001. 13(14): p. 1090-+.

10. See, K.H., et al., *A reactive core-shell nanoparticle approach to prepare hybrid nanocomposites: effects of processing variables.* Nanotechnology, 2005. 16(9): p. 1950-1959.

11. Hirsch, L.R., et al., *Metal nanoshells.* Ann Biomed Eng, 2006. 34(1): p. 15-22.

12. Preston, T.C. and R. Signorell, *Growth and Optical Properties of Gold Nanoshells Prior to the Formation of a Continuous Metallic Layer.* Acs Nano, 2009. 3(11): p. 3696-3706.

13. Westcott, S.L., et al., *Formation and adsorption of clusters of gold nanoparticles onto functionalized silica nanoparticle surfaces.* Langmuir, 1998. 14(19): p. 5396-5401.

14. Salgueirino-Maceira, V., F. Caruso, and L.M. Liz-Marzan, *Coated colloids with tailored optical properties.* Journal of Physical Chemistry B, 2003. 107(40): p. 10990-10994.

15. Penkova, A., et al., *Gold nanoparticles on silica monospheres modified by amino groups.* Microporous Mesoporous Mater, 2009. 117: p. 530-534.

16. Phonthammachai, N., et al., *Synthesis of contiguous silica-gold core-shell structures: critical parameters and processes.* Langmuir, 2008. 24(9): p. 5109-12.

17. Stober, W., A. Fink, and E. Bohn, *Controlled Growth of Monodisperse Silica Spheres in Micron Size Range.* Journal of Colloid and Interface Science, 1968. 26(1): p. 62-&.

18. Liu, G., et al., *Preparation of silica/polymer hybrid microspheres and the corresponding hollow polymer microspheres with functional groups.* Polymers For Advanced Technologies, 2008. 19: p. 1922-1930.

19. Lu, Q., et al., *Tuning of the vinyl groups' spacing at surface of modified silica in preparation of high density imprinted layer-coated silica nanoparticles: a dispersive solid-phase extraction materials for chlorpyrifos.* Talanta, 2010. 81(3): p. 959-66.

20. claesson, E.M. and A.P. Philipse, *Thiol-functionalized silica colloids, grains, and membranes, for irreversible adsorption of metal(oxide) nanoparticles.* Colloids and Surfaces a-Physicochemical and Engineering Aspects, 2007. 297: p. 46-54.

21. Badley, R.D., et al., *Surface Modification of Colloidal Silica.* Langmuir, 1990. 6(4): p. 792-801.

22. Chen, S., et al., *Novel One-pot Sol-Gel Preparation of Amino-functionalized Silica Nanoparticles.* Chemistry Letters, 2008. 37(11): p. 1170-1171.

23. Bourgeat-Lami, E., et al., *Designing Organic/Inorganic Colloids by Heterophase Polymerization.* Macromolecular Symposia, 2007. 248: p. 213-226.

24. Lapeyre, V., et al., *Multiresponsive hybrid microgels and hollow capsules with a layered structure.* Langmuir, 2009. 25(8): p. 4659-67.

25. Brinson, B.E., et al., *Nanoshells made easy: improving Au layer growth on nanoparticle surfaces.* Langmuir, 2008. 24(24): p. 14166-71.

26. White, N.P.a.T.J., *One-Step Synthesis of Highly Dispersed Gold Nanocrystals on Silica Spheres.* Langmuir, 2007. 23(23): p. 11421-11424.

27. Bergna, H. and W.O. Roberts, *Colloidal silica: fundamentals and applications*. Surfactant Science Series. 2006, Boca Raton: CRC Press Taylor and Francis Group. 855.

28. Ken-Tye Yong, M.T.S., Hong Ding, Paras N. Prasad, *Preparation of Gold Nanoparticles and their Applications in Anisotropic Nanoparticle Synthesis and Bioimaging.* Plasmonics, 2009. 4: p. 79-93.

29. Chang, C.K., Y.J. Chen, and C.T. Yeh, *Characterizations of alumina-supported gold with temperature-programmed reduction.* Applied Catalysis a-General, 1998. 174(1-2): p. 13-23.

30. Kung, H.H., M.C. Kung, and C.K. Costello, *Supported Au catalysts for low temperature CO oxidation.* Journal of Catalysis, 2003. 216(1-2): p. 425-432.

31. Kim, J., et al., *Designed fabrication of multifunctional magnetic gold nanoshells and their application to magnetic resonance imaging and photothermal therapy.* Angewandte Chemie-International Edition, 2006. 45(46): p. 7754-7758.

32. Hanprasopwattana, A., et al., *Titania coatings on monodisperse silica spheres (characterization using 2-propanol dehydration and TEM).* Langmuir, 1996. 12(13): p. 3173-3179.

33. Liu, Z.X., et al., *Fabrication and near-infrared photothermal conversion characteristics of Au nanoshells.* Applied Physics Letters, 2005. 86(11): p. -.

34. Jain, P.K., et al., *Review of some interesting surface plasmon resonance-enhanced properties of noble metal nanoparticles and their applications to biosystems.* Plasmonics, 2007. 2(3): p. 107-118.

35. Eustis, S. and M.A. El-Sayed, *Why gold nanoparticles are more precious than pretty gold: Noble metal surface plasmon resonance and its enhancement of the radiative and nonradiative properties of nanocrystals of different shapes.* Chemical Society Reviews, 2006. 35(3): p. 209-217.

36. Mie, G., *Articles on the optical characteristics of turbid tubes, especially colloidal metal solutions.* Annalen Der Physik, 1908. 25(3): p. 377-445.

37. Kelly, K.L., et al., *The optical properties of metal nanoparticles: The influence of size, shape, and dielectric environment.* Journal of Physical Chemistry B, 2003. 107(3): p. 668-677.

38. Jain, P. and M.A. El-Sayad, *Plasmonic coupling in noble metal nanostructures.* Chemical Physics Letters, 2010. 487: p. 153-164.

39. Oldenburg, S.J., et al., *Nanoengineering of optical resonances.* Chemical Physics Letters, 1998. 288(2-4): p. 243-247.

40. Peceros, K.E., et al., *Dipole-dipole plasmon interactions in gold-on-polystyrene composites.* Journal of Physical Chemistry B, 2005. 109(46): p. 21516-20.

41. Storti, B., et al., *One-Pot Synthesis of Gold Nanoshells with High Photon-to-Heat Conversion Efficiency.* Journal of Physical Chemistry C, 2009. 113(18): p. 7516-7521.

42. O'Neal, D.P., et al., *Photo-thermal tumor ablation in mice using near infrared-absorbing nanoparticles.* Cancer Lett, 2004. 209(2): p. 171-6.

43. Cole, J.R., et al., *Photothermal Efficiencies of Nanoshells and Nanorods for Clinical Therapeutic Applications.* Journal of Physical Chemistry C, 2009. 113(28): p. 12090-12094.

44. Gobin, A.M., et al., *Near infrared laser-tissue welding using nanoshells as an exogenous absorber.* Lasers Surg Med, 2005. 37(2): p. 123-9.

45. Khlebtsov, B. and N. Khlebtsov, *Enhanced solid-phase immunoassay using gold nanoshells: effect of nanoparticle optical properties.* Nanotechnology, 2008. 19(43): p. -.

46. Loo, C., et al., *Immunotargeted nanoshells for integrated cancer imaging and therapy.* Nano Letters, 2005. 5(4): p. 709-11.

47. Hirsch, L.R., et al., *Nanoshell-mediated near-infrared thermal therapy of tumors under magnetic resonance guidance.* Proceedings of the National Academy of Sciences of the United States of America, 2003. 100(23): p. 13549-13554.

48. Hirsch, L.R., et al., *Nanoshell-Assisted Tumor Ablation Using near Infrared Light under Magnetic Resonance Guidance.* Proc Natl Acad Sci U S A, 2003. 100: p. 13549-13554.

49. Harris, N., M.J. Ford, and M.B. Cortie, *Optimization of plasmonic heating by gold nanospheres and nanoshells.* Journal of Physical Chemistry B, 2006. 110(22): p. 10701-7.

50. Zha, L.S., et al., *Monodisperse temperature-sensitive microcontainers.* Advanced Materials, 2002. 14(15): p. 1090-+.

51. Coutinho, C.A., et al., *Novel ceria-polymer microcomposites for chemical mechanical polishing.* Applied Surface Science, 2008. 255(5): p. 3090-3096.

52. Duff, D.G., A. Baiker, and P.P. Edwards, *A New Hydrosol of Gold Clusters .1. Formation and Particle-Size Variation.* Langmuir, 1993. 9(9): p. 2301-2309.

53. Duff, D.G., et al., *A New Hydrosol of Gold Clusters .2. A Comparison of Some Different Measurement Techniques.* Langmuir, 1993. 9(9): p. 2310-2317.